Cell and Tissue Research
https://doi.org/10.1007/s00441-024-03932-4

RESEARCH

TNBS colitis induces architectural changes and alpha-synuclein overexpression in mouse distal colon: A morphological study

Arianna Casini[1] · Giorgio Vivacqua[2] · Ludovica Ceci[1] · Stefano Leone[1] · Rosa Vaccaro[1] · Marco Tagliafierro[1] · Filippo Maria Bassi[1] · Sara Vitale[1] · Emanuele Bocci[1] · Luigi Pannarale[1] · Simone Carotti[2] · Antonio Franchitto[3] · Patrizia Mancini[4] · Roberta Sferra[5] · Antonella Vetuschi[5] · Giovanni Latella[6] · Paolo Onori[1] · Eugenio Gaudio[1] · Romina Mancinelli[1]

Received: 24 September 2024 / Accepted: 11 November 2024

Abstract

Alpha-synuclein (α-syn) is widely expressed in presynaptic neuron terminals, and its structural alterations play an important role in the pathogenesis of Parkinson's disease (PD). Aggregated α-syn has been found in brain, in the peripheral nerves of the enteric nervous system (ENS) and in the intestinal neuroendocrine cells during synucleinopathies and inflammatory bowel disorders. In the present study, we evaluated the histomorphological features of murine colon with 2,4,6-trinitrobenzene sulfonic acid (TNBS)-induced colitis, a common model of colitis. Thereafter, we investigated the expression of α-syn, Toll-like receptor 4 (TLR4), choline acetyltransferase (ChAT), vasoactive intestinal peptide (VIP), tyrosine hydroxylase (TH), calcitonin gene-related peptide (CGRP), and calcitonin-like receptor (CALCR). Finally, we investigated the presence of phosphorylated α-syn (pS129 α-syn) aggregates and their relationship with inflammatory cells. Colon from TNBS mice showed an increase in inflammatory cells infiltrate and significative changes in the architecture of the intestinal mucosa. α-Syn expression was significantly higher in inflamed colon. VIP was increased in both the mucosa and muscularis externa of TNBS mice, while TH, CGRP, and CALCR were significantly reduced in TNBS mice. Amyloid aggregates of pS129 α-syn were detectable in the ENS, as in the macrophages around the glands of the mucosa correlating with the markers of inflammation. This study describes — for the first time — the altered expression of α-syn and the occurrence of amyloid α-syn aggregates in the inflammatory cells under colitis, supporting the critical role of bowel inflammation in synucleinopathies and the involvement of α-syn in IBD.

Keywords Alpha-synuclein · Enteric nervous system · Colitis · Gut-brain axis · Inflammatory bowel disease

Abbreviations

α-Syn	Alpha-synuclein
α-syn	Alpha-synuclein
PD	Parkinson's disease
ENS	Enteric nervous system
TNBS	2,4,6-Trinitrobenzene sulfonic acid
TLR4	Toll-like receptor 4
ChAT	Choline acetyltransferase
VIP	Vasoactive intestinal peptide
TH	Tyrosine hydroxylase

Arianna Casini and Giorgio Vivacqua contributed equally to this work.

✉ Romina Mancinelli
romina.mancinelli@uniroma1.it

[1] Department of Anatomical, Histological, Forensic Medicine and Orthopaedics Sciences, Sapienza University of Rome, Via Alfonso Borelli 50 – 00161, Rome, Italy

[2] Integrated Research Center (PRAAB), Campus Biomedico University of Rome, Rome, Italy

[3] Division of Health Sciences, Department of Movement, Human and Health Sciences, University of Rome Foro Italico, Rome, Italy

[4] Department of Experimental Medicine, Sapienza University of Rome, Rome, Italy

[5] Department of Biotechnological and Applied Clinical Sciences, University of L'Aquila, L'Aquila, Italy

[6] Division of Gastroenterology, Hepatology and Nutrition, Department of Life, Health & Environmental Sciences, San Salvatore Hospital, University of L'Aquila, L'Aquila, Italy

Published online: 10 December 2024

CGRP	Calcitonin gene related peptide
CALCR	Receptor calcitonin-like receptor
IHC	Immunohistochemistry
IF	Immunofluorescence
pS129 α-syn	Phosphorylated α-syn
ThT	Thioflavin T
IBD	Inflammatory bowel diseases
CD	Crohn's disease
UC	Ulcerative colitis
DSS	Dextran sulfate sodium
H&E	Hematoxylin and eosin
PAS	Periodic acid Schiff
PBS	Phosphate-buffered saline
HRP	Horseradish peroxidase
DAB	Diaminobenzidine
DAPI	4′,6-Diamidino-2-phenylindole
OM	Optical magnification
6-OHDA	6-Hydroxydopamine
MPTP	1-Methyl-4-phenyl1-1,2,3,6-tetrahydropyridine
ON	Overnight

Introduction

IBD are chronic GI disorders including Crohn's disease (CD) and ulcerative colitis (UC) (Vaccaro et al. 2023), characterized by bowel inflammation and dramatic changes in bowel histomorphology. Increased expression of α-syn in colonic mucosa has been reported in patients with UC as well as in DSS-induced colitis in rats (Espinosa-Oliva, et al. 2024). Moreover, CD's patients showed a 2.35-fold increase of α-syn expression in inflamed intestinal areas compared to healthy subjects (Prigent, et al. 2019b). Therefore, the studies presented thus far in IBD patients are consistent with the evidence that inflammation in the gut could promote in situ α-syn aggregation, which may lead to α-syn pathology in the brain.

α-Syn is a 140-aminoacid protein richly expressed at the pre-synaptic terminals and in nerve cells' nuclei, both in the central and peripheral nervous system. Several studies support its crucial role in neurotransmitter release and in synaptic vesicle pool homeostasis (Anwar, et al. 2011, Bonaccorsi di Patti, et al. 2022, Casini, et al. 2021, Cheng, et al. 2011, Lashuel, et al. 2013, Spillantini and Goedert 2018, Vivacqua, et al. 2014). In physiological conditions, it is mainly found as a monomer (Vivacqua, et al. 2016, 2019) and preferentially binding to lipid membranes and synaptic vesicles (Middleton and Rhoades 2010). Conversely, α-syn misfolding and aggregation are considered the pathological hallmarks of PD and other diseases, including dementia with Lewy bodies and multiple system atrophy (Kakimoto, et al. 2023, Woerman, et al. 2018).

Due to the possible formation — under inflammatory conditions — of α-syn aggregates in the gut and to their possible spread from the gut to the brain (Bottner, et al. 2015, Van Den Berge, et al. 2019), bowel inflammation is acquiring increasing interest in synucleinopathies. In particular, TLR4 would play a central role on the intertwined relation between α-syn aggregation in the gut and neurodegeneration, since it may act as a receptor for the internalization of α-syn aggregates, increasing gut permeability and inflammation and thereby driving to the neuroinflammatory process in the brain (Shao, et al. 2019). Despite such evidence, very few studies have systematically analyzed the expression of α-syn and the occurrence of α-syn aggregates in the gut, in relation to molecular and morpho-functional alterations during IBD or experimental colitis.

In the present study, we aim to evaluate how inflammation of the colon could affect the architecture of the colonic ENS, investigated by the analysis of ChAT, as marker of cholinergic enteric neurons (Kurnik, et al. 2015; Vaccaro, et al. 2016), TH, as marker of dopaminergic and catecholaminergic neurons (Hoover, et al. 2014), VIP, as marker of enteric submucosal neurons (Brehmer, et al. 2006), as well as CGRP and its receptor, which are mainly expressed by intrinsic primary afferent enteric neurons (Hibberd, et al. 2022). Moreover, the expression and the eventual aggregation of α-syn, as well as the expression of TLR4, which has been reported as a possible cellular receptor for α-syn and its internalization (Nishitani, et al. 2024) are evaluated. The intertwined relations between inflammation, α-syn aggregation and neuroendocrine mediators provide a more detailed knowledge about the gut-to-brain interactions and their potential role in α-syn-mediated neurodegeneration, highlighting also the possible role of α-syn in bowel mobility, inflammation, and neuroendocrine function in the context of IBD.

Material and methods

Animal models

Ten healthy adult mice, (Black Swiss × 129SVJ strain) 5 weeks of age, were included in the protocol study. All mice were maintained in a specific pathogen-free facility with controlled light and dark cycles of 12 h each, at 23 °C controlled temperature, fed with standard rodent chow pellets (Laboratori Piccioni, Gessate, Milan, Italy). Mice were kept in microisolator cages and allowed free access to food and water. The study protocol was approved by the Animal Research Committee of the University of L'Aquila, Italy.

Induction of colitis

Colitis was induced in 5 mice by weekly intrarectal administration of TNBS (Sigma Aldrich, Milan, Italy) under light anesthesia according to the method previously reported (Latella, et al. 2009). Each mouse received an incremental dose of TNBS over a 6-week period. At weeks I and II, mice received 0.5 mg of TNBS in 30% ethanol; at weeks III and IV, mice received 0.75 mg of TNBS in 45% ethanol; and at weeks V and VI, mice received 1.0 mg of TNBS in 45% ethanol. The solution of TNBS-ethanol was administered in a total volume of 100 µL through a medical-grade polyurethane tube (diameter, 1 mm) the tip of which was positioned at 3 cm beyond the anus. Five mice in the control group received 100 µL of 0.9% saline instead of TNBS by enema. Five days after the last TNBS administration (week VI), the animals of each group were euthanized by cervical dislocation under deep CO_2 anesthesia and underwent laparotomy (Fig. 1). The protocol was performed in adherence of the authors to the Italian National Research Council criteria for care and use of laboratory animals.

Colon sample recovery and preparation

We used and completed the experimental study protocol with 5 in the TNBS group and 5 in the control group, respect to the original twenty samples. After laparotomy, the distal colon was visualized and rapidly dissected. The colon was then placed in a Petri dish containing sterile saline solution. After being opened with a longitudinal section, it was rinsed with a sterile saline solution and subsequently attached to a wooden tongue depressor, for the inspection of macroscopic lesions. The colon was then cut into segments and fixed in 4% buffered formaldehyde and embedded in paraffin for histological and immunohistochemical assays, (Fig. 1).

Histomorphology

Paraffin-embedded sections were cut at 4-µm thickness and stained with hematoxylin and eosin (H&E) for morphological analysis of each group of mice. Tissue samples were evaluated by score of (i) inflammatory cell infiltration (scores 0–3) and (ii) mucosal architecture considering epithelial changes and tissue damage (epithelial defects, connective tissue repair, non-parallel, and variable crypts) (scores 0–3). Pathology scores were as follows: 0, no significant changes (0%); 1, minimal (< 10%); 2, mild (10–25%); 3, moderate (25–40%); 4, marked (40–50%); and 5, severe (> 50%) (Bechtold, et al. 2024; Erben, et al. 2014). Next, periodic acid Schiff (PAS) staining and Alcian blue staining were used to characterize the variations in goblet cells and the possible chemical alterations of mucin secretion. The staining procedure to evaluate the basic

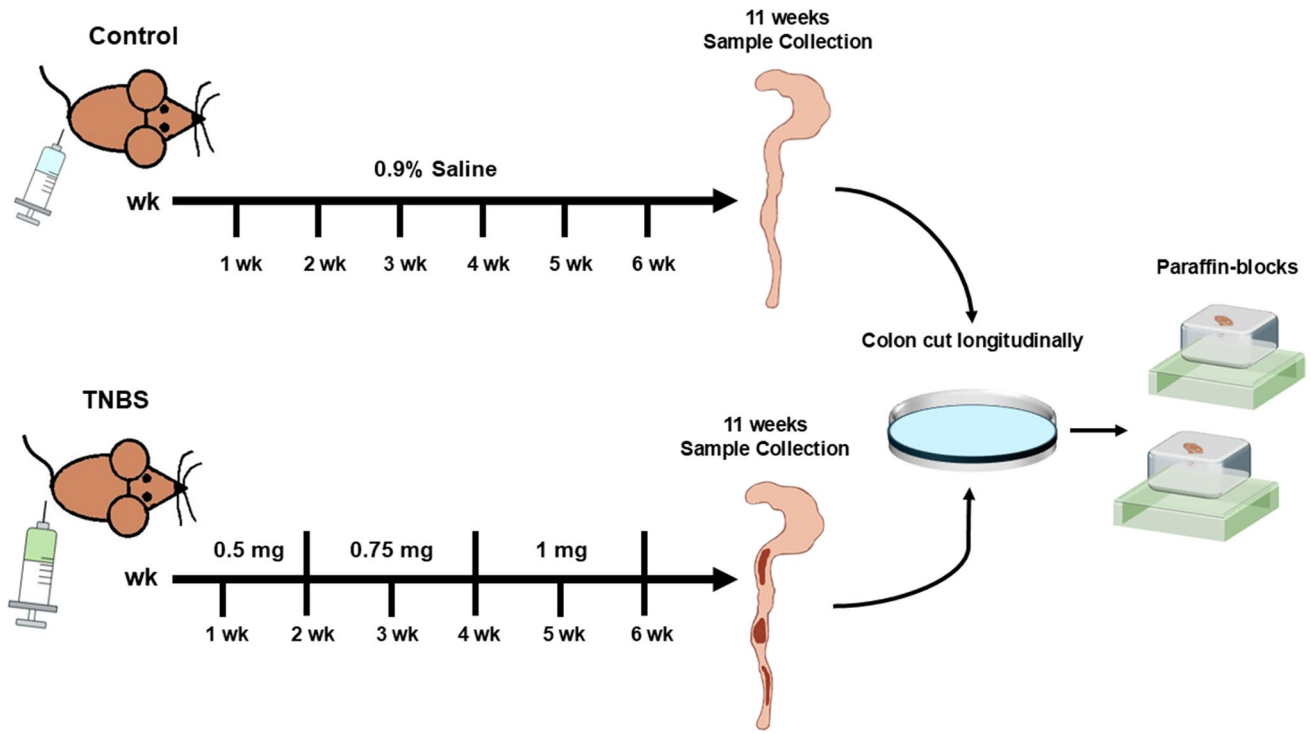

Fig. 1 Experimental design of TNBS-induced colitis in mice

mucous secretion involved sample deparaffinization with xylene and rehydration with graded ethanol, followed first by incubation with 1% periodic acid, and subsequently incubated with Schiff's reagent (477591- Carlo Erba Reagents S.A.S). The sections were counterstained with Mayer's hematoxylin, dehydrated with ethanol and cleared with xylene before mounting and visualizing (Machorro-Rojas, et al. 2019). In the next staining to evaluate acidic mucins, subsequent deparaffinization and rehydration, sections were incubated firstly with Alcian blue solution (pH 2,5) according to Mowry, and then with sodium tetraborate solution and in the end with carmallum, according to Mayer (Machorro-Rojas et al. 2019). Furthermore, we performed silver impregnation to characterize nervous fibers and collagen fibers. Colonic sections were pre-treated as in the previous staining. The samples were subjected to an equimolar mixture of a potassium permanganate solution and an acid activation buffer for preparatory oxidation. The specimens underwent washing with distilled water to prepare them for treatment with an oxalic acid solution. After washing, the sections were treated with ferric ammonium sulfate, to allow the binding of the substance to argyrophilic structures. Then, the samples were treated with an ammoniacal silver solution which replaced iron previously bound to tissues. After washing, the sections were treated with a neutral formalin solution acting as a reducing agent to remove oxygen from the trivalent iron (ferric ammonium sulfate), thereby releasing metallic silver which deposits from argyrophilic structures. After a double wash, sodium thiosulfate hyposulfite was used as fixing agent and to remove the unreduced silverdiamine cation. At the end, all the sections were dehydrated with ethanol and cleared with xylene before mounting. A colon section represents one mouse. We scanned all the colon section by the Leica Aperio CS2 (Aperio Scanscope CS System, Leica Biosystems, Milan, Italy). The scanned section was analyzed with ImageScope × 64 software 12.4.6 with a specific algorithm. The algorithm will select the positive staining (brown for IHC and purple-magenta color for PAS) and the negative staining. At last, we applied the following formula: number of positive/ total number (positive + negative) × 100. Hence, each dot in the dot-graph showed the colon of one mouse of the experimental design.

IHC

Paraffin-distal colon sections (4 µm) were processed for immunohistochemistry (IHC), as following: after the incubation in 3% H_2O_2 for 20 min to dampen the endogenous peroxidase activity, distal colon sections were treated with antigen retrieval (10 mM sodium citrate buffer, pH 6.0, H3300, Vector Laboratories, Burlingame, CA, USA) for 30 min at 90 °C. Sections were incubated with the primary antibody overnight (ON) at 4 °C in a humidified chamber (Table 1). Following washing with 1 × phosphate-buffered saline (PBS) three times for 5 min each, the secondary antibody labeled with horseradish peroxidase (HRP) polymer were applied for 45 min in a humidified chamber at room temperature. The secondary antibodies used were the Dako Envision + System-HRP labeled polymer anti-rabbit (K4003, Agilent Technologies, CA, USA) and ImmPRESS Horse anti-goat IgG polymer reagent (MP-7405, Vector Laboratories, Burlingame, CA, USA). Distal colonic sections were washed 3 times with 1 × PBS, and covered with diaminobenzidine (Dako, Liquid DAB + Substrate Chromogen System, K3468, Agilent Technologies, CA, USA) from 10 s to few minutes, and signal development was monitored under the microscope (Leica DMLB Clinical Microscope). Sections were counterstained with hematoxylin staining for 45 s and then mounted and cover slipped. All the stained slides were scanned with Leica Aperio CS2 (Aperio Scanscope CS System, Leica Biosystems, Milan, Italy) and quantified with ImageScope × 64 software 12.4.6 with a specific algorithm. Briefly, we selected the area of colon to analyze, and then

Table 1 List of primary antibodies

Antibodies	Application	Description	Dilution	Cat. no	Company
α-Syn	IHC	Monoclonal rabbit	1:200 ON	E4U2F	Cell signaling
TLR4	IHC/IF	Polyclonal rabbit	1:100 ON	PA5-23,124	Invitrogen
ChAT	IHC/IF	Polyclonal goat	1:100 ON	AB144P	Sigma-Aldrich
α-Syn	IF	Polyclonal chicken	1:500 ON	PA5-143,581	Invitrogen
VIP	IHC	Polyclonal rabbit	1:800 ON	7854/01-B5	Euro-Diagnostica
TH	IHC	Polyclonal rabbit	1:500 ON	AB152	Sigma-Aldrich
CGRP	IHC	Polyclonal rabbit	1:400 ON	AB47027	Abcam
CALCRL	IHC	Polyclonal rabbit	10ug/mL ON	LS-A6731	LS-Bio
α-Syn (pS129)	IF	Monoclonal rabbit	1:300	AB51253	Abcam
F4/80	IF	Monoclonal rat	1:200	sc-52664	Santa Cruz Biotechnology

we run the algorithm which detected the positive staining (brown/strong positive) and the non-positive area. Next, we measured the % of positive area (brown staining) by dividing the positive area for total area (strong positive and non-positive areas) and multiply per 100.

IF

The immunofluorescence (IF) protocol was used to assess the expression and the colocalizations: α-syn/TLR4, α-syn/ChAT, α-syn/VIP as well as to detect the occurrence of pS129 α-syn aggregates in TNBS-treated colon, their possible amyloid conformation assessed with thioflavin T (ThT) staining and their possible localization in the context of inflammatory phagocytic cells, assessed by macrophage markers (F4/80 as pan-macrophage marker). Paraffin-distal colon sections (4 µm) were treated with antigen retrieval (10 mM sodium citrate buffer, pH 6.0, H3300, Vector Laboratories, Burlingame, CA, USA) for 30 min 90 °C. After washing 3 times in 0.01% PBS-Tween for 5 min, the sections were incubated with 5% bovine serum albumin (BSA) for 1 h at room temperature to prevent non-specific protein binding. Sections were incubated with primary antibodies ON at 4 °C in a humidified chamber. Following washing with 0.01% PBS-Tween three times for 5 min each, sections were incubated for 1 h at room temperature with labeled isotype-specific secondary antibodies fluorescent-dye conjugated (Table 2). The samples were then counterstained with 4,6-diamidino-2-phenylindole (DAPI) (UltraCruz aqueous mounting medium with DAPI, sc-24941, Santa Cruz Biotechnology, Inc., Dallas, TX, USA) to allow the visualization of cell nuclei. The stained slides were analyzed using Leica Microsystems DM 4500 B Fluorescence Microscopy (Wetzlar, Germany) equipped with a JenoptikProg Res C10 Plus Videocam (Jena, Germany)

Table 2 List of secondary antibodies

Antibodies	Application	Description	Cat. No	Company
Anti-rabbit	IF	Alexa Fluor ™ 488	A-21206	ThermoFisher Scientific
Anti-chicken	IF	Alexa Fluor™ 488	A-11039	ThermoFisher Scientific
Anti-rat	IF	Alexa Fluor™ 488	A-11006	ThermoFisher Scientific
Anti-rabbit	IF	Alexa Fluor™ 594	A-11012	ThermoFisher Scientific
Anti-goat	IF	Alexa Fluor™ 594	A-21468	ThermoFisher Scientific

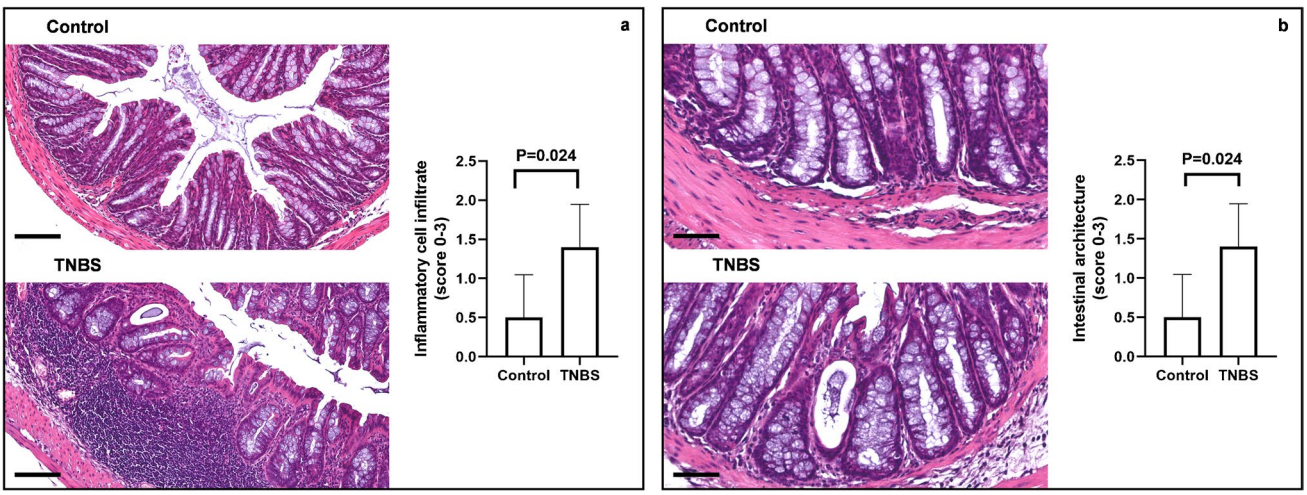

Fig. 2 Histological alterations in the TNBS-induced colitis. Representative images of H&E-staining of colon tissue showing changes in (**a**) inflammatory cell infiltrates and in (**b**) intestinal architecture between controls and TNBS-treated mice compared to controls. Colonic samples from control mice showed normal appearance with absence of inflammation (**a**) and typical architecture (**b**). Following TNBS treatment, the colon specimens displayed a marked increase of inflammatory infiltrate in lamina propria and submucosa layer compared to control mice. The intestinal architecture was changed in the colon of TNBS-treated-mice, displaying crypt dilatation or depletion, as well as branching and destroyed crypts in comparison to control mice. Optical magnification (OM) of inflammatory cell infiltrate = 20×, scale bars = 100 µm. OM of intestinal architecture images = 40×, scale bars = 50 µm

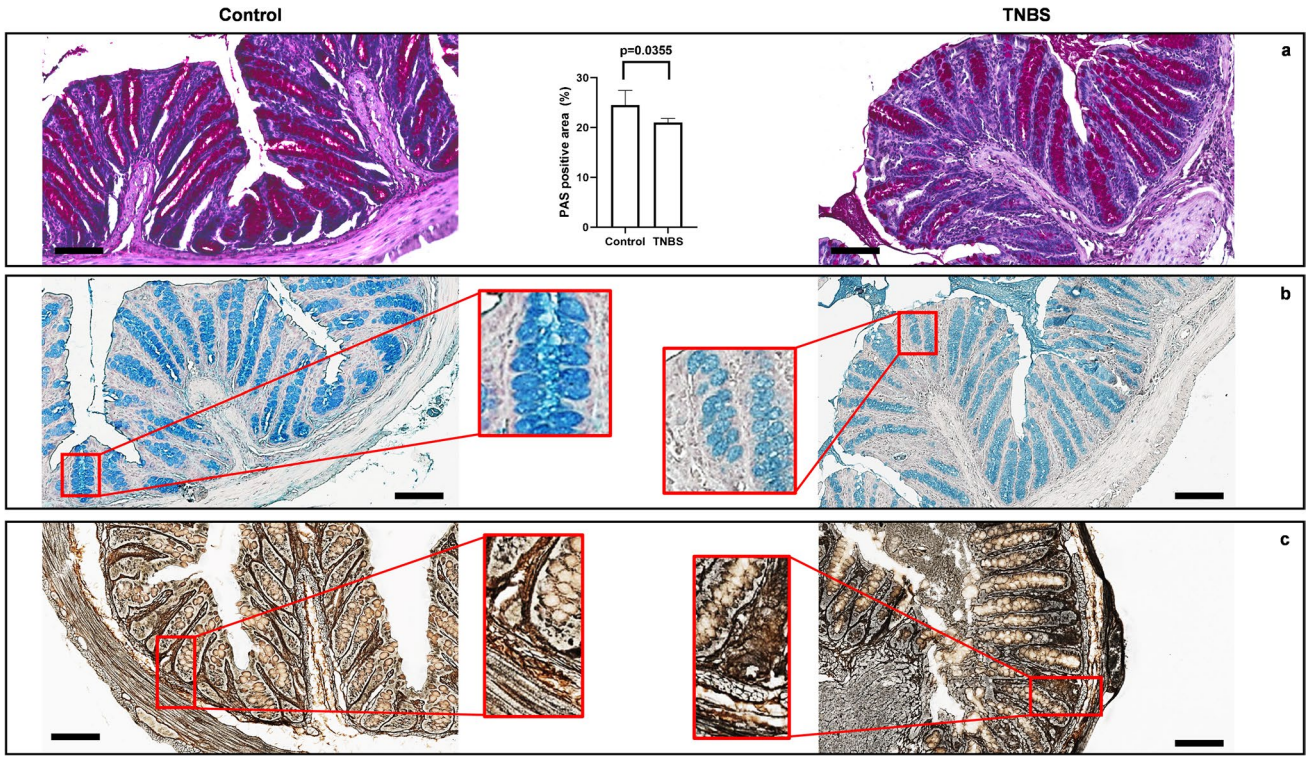

Fig. 3 Goblet cells and myenteric plexuses are altered after TNBS-induced colitis. (**a**) TNBS-treated mice show significant reduction of basic mucus-secreting goblet cells, as detected by PAS staining, compared to control mice (*SD* for control = 2.934; *SD* for TNBS = 0.819; *p*-value = 0.0355). (**b**) Alcian blue staining (employed to evaluate the acidic mucin-secreting goblet cells) shows a decrease in the Alcian blue staining intensity in TNBS treated mice, in comparison with control mice. (**c**) Silver impregnation (SI) staining shows the changes and the degeneration of enteric neuronal structures in the colonic wall of TNBS-treated mice, in comparison to control mice, as clearly demonstrated by the increased amount of argyrophilic elements detected in the colon of TNBS mice in comparison to control mice (enlarged squared panels). OM of PAS, Alcian blue and silver staining: 20×, scale bars = 100 µm

and analyzed with Leica Application Suite X (LAS X) for Life Science (Leica Microsystems). In addition, we used an Axio Observer Z1 inverted microscope, equipped with an ApoTome.2 System (Carl Zeiss Inc., Ober Kochen, Germany). The ApoTome system provided an optical section of fluorescent samples, calculated from three images with different grid positions without time lag. Digital images were acquired with the Camera Axiocam 807 mono (Zeiss) and processed with the ZEN 3.8 Pro software (Zeiss).

Quantification and statistical analysis

GraphPad Prism 8.3.1 software (San Diego, CA) was used to perform the statistical analyses. Data are expressed as the *means* ± *SD*, as previously shown in IHC section. Differences between groups were evaluated by the student unpaired *t* test when 2 groups were analyzed. A value of $p < 0.05$ was considered statistically significant.

Results

Morphological changes of distal colon after TNBS treatment

Basal lymphoepithelial infiltrations, branching and destroyed crypts, and congested blood vessels in the lamina propria were found in the colon from TNBS-treated mice. Furthermore, inflammatory lymphocytic infiltrate in the lamina propria extending to the mucosa and the submucosa, dilation of the crypts, and crypts abscesses were observed. No morphological changes were observed in the colon from control mice (Fig. 2a, b). We evaluated the presence of goblet cells and mucins by PAS and Alcian blue staining. TNBS promoted a significant depletion of basic mucin-producing goblet cells in the distal colon, as detected by a significative loss of PAS-positive cells in comparison to control mice (Fig. 3a). Next, we morphologically observed that TNBS-treated mice showed a paler staining for acid mucin producing cells, as investigated with Alcian blue staining, in comparison to the colon

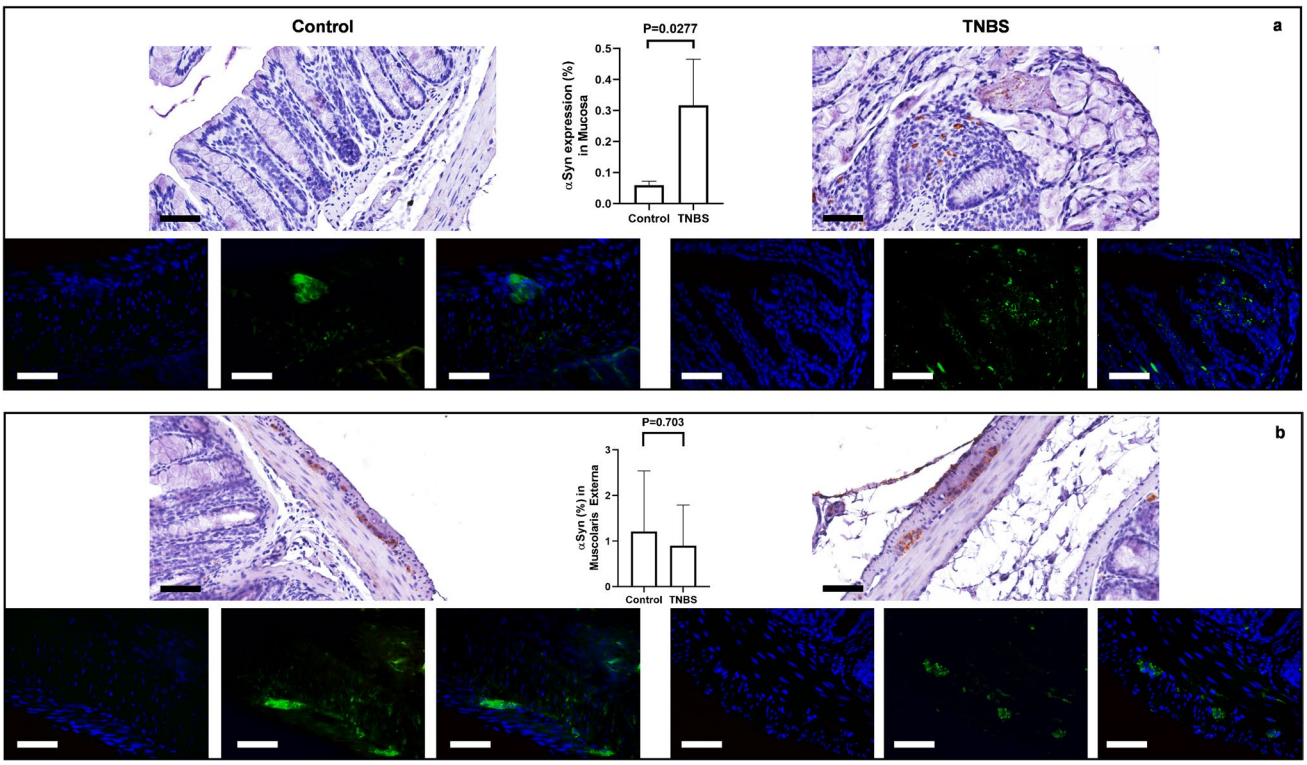

Fig. 4 α-Syn expression is altered in TNBS-induced colitis. (**a**) In control mice, α-syn was localized in scattered cells of the lamina propria, placed around the crypts. Following the treatment with TNBS, the expression of α-syn was significantly increased in the mucosa with the presence of immunoreactive varicous fibers and peri-glandular cells at the level of lamina propria. *SD* for control = 0.0121; *SD* for TNBS = 0.1488; *p*-value = 0.0277. (**b**) In control mice, α-syn was expressed in the ganglia of the myenteric plexus where it discloses a homogenous and compact staining in neuronal cells. In TNBS-treated mice, the ganglia of the myenteric plexus disclose a morphologically altered positivity with α-syn expression characterized by a punctate and scattered staining in the context of the enteric neuronal cells. Quantitative analysis (linear bars with individual dots) confirmed that α-syn-immunoreactivity was significantly increased in the mucosa of TNBS-treated mice, in comparison to control mice, whereas not significant differences were detected in the expression of α-syn by the ganglia of the myenteric plexus between TNBS-treated and control mice. *SD* for control = 1.332; *SD* for TNBS = 0.8939; *p*-value = 0.703. OM 40× — scale bars = 50 μm

of control mice (Fig. 3b). Silver staining was used to evaluate the alteration in the morphology of the ENS after TNBS treatment. The ganglia in both the submucosal and the myenteric plexuses were compared in TNBS-treated and control mice. In control mice, the ganglia disclosed a well-structured and defined morphology with neurons characterized by rounded nuclei with defined nuclear envelope. The silver staining was increased and less defined when degeneration of neurons and glial cells created a dysmorphic architecture of the enteric plexa. Indeed, in the colon of the TNBS-treated mice, we found a disorganized architecture of the enteric nervous elements, as detected by the increased and less defined argyrophilic staining in comparison to control mice (Fig. 3c).

TNBS altered α-syn expression in distal mouse colon

α-Syn-immunoreactivity (ir) was higher in the colon from TNBS-treated mice in comparison to control mice. Expression was ubiquitous in the intestinal wall of the distal colon. Specifically, it was detectable in the cells and nerve fibers around the crypts, in the ganglia of both submucosal and myenteric plexa and in the varicose nerve fibers of the myenteric plexus. Quantification of α-syn expression displayed regional differences. Indeed, TNBS-treated mice showed increased expression of α-syn in the peri-glandular cells of the mucosa when compared to control mice (Fig. 4a, upper panel). No significant changes in the myenteric plexus and in the circular muscular layer were found (Fig. 4b, lower panel). This phenotype was also confirmed by IF. Indeed, an increased expression of α-syn was detectable in the peri-glandular cells and mucosal fibers (Fig. 4a, upper panel), whereas the expression in the ganglia of the myenteric plexus looked comparable in TNBS-treated and control mice (Fig. 4b, lower panel), with the presence of some morphological differences in the staining: α-syn IF appeared homogenous and

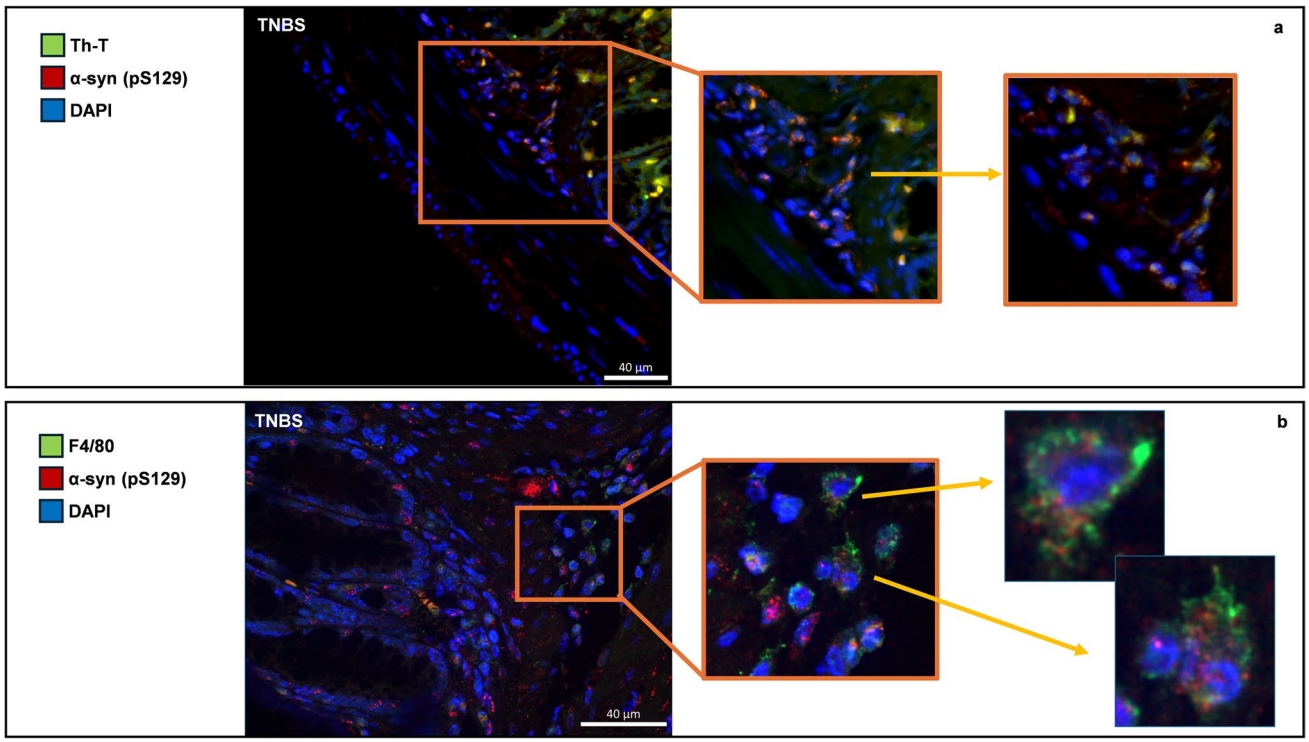

Fig. 5 (**a**) IF showing ThT (green) and pS129 α-syn (red) in the colonic wall of TNBS mice. ThT increases in fluorescence upon binding to amyloid fibrils, and its presence was higher in inflamed intestine together with pS129 α-syn, a widely described marker of amyloid aggregation. Aggregates of α-syn (**b**) double IF for pS129 α-syn (red) and F4/80 pan-macrophagic marker (green) in the distal colon of TNBS-treated mice. Large aggregates of pS129 α-syn are detectable in the mucosa of the distal colon after TNBS treatment, and they extensively co-expressed with macrophages placed around the colonic glands. Aggregates of pS129 α-syn are evident in the context of these cells where they form clusters of dot-like staining in the cytoplasm and around the nucleus. OM 20×. Scale bars 40 µm

well defined in the ganglia of control mice, whereas it appeared punctuated and scattered in the myenteric neurons of TNBS-treated mice.

Double IF for pS129 α-syn and the pan-macrophagic marker F4/80 demonstrate the presence of widely distributed aggregates of α-syn in the colon of TNBS-treated mice, localized either in the mucosa, as in myenteric neurons (Fig. 5b). The pS129 α-syn positive structures co-express with F4/80 in the submucosa and inflammatory infiltrate around mucous glands, indicating the presence of α-syn aggregates in mononuclear cells during TNBS-mediated colitis (Fig. 5b). Furthermore, the same aggregates co-expressed with ThT in the same areas, supporting their amyloid conformation (Fig. 5a).

TNBS altered TLR4 expression in distal colon

Cell-to-cell transmission of α-syn can occur by both receptor-mediated (Zhang, et al. 2021) and non-receptor mediated mechanisms (Lee, et al. 2008). Moreover, TLR4, closely associated with inflammation, has been also considered a possible receptor for the endocytosis and the cellular internalization of α-syn and α-syn aggregates (Nishitani et al. 2024). Double IF revealed co-localization between TLR4 and α-syn in the colonic mucosa and in the myenteric plexus. In control mice, IF confirmed the high expression of TLR4 in the enterocytes, without evident colocalization with α-syn (Fig. 6a). Expression of both TLR4 and α-syn was evident in the neurons of the myenteric plexus, where slight spots of co-expression were detectable (Fig. 6b). After TNBS-treatment, the colocalization between TLR4 and α-syn appeared strongly increased in both peri-glandular inflammatory cells of the lamina propria and enterocytes in the mucosa (Fig. 6c), as well as in the ganglia of the myenteric plexus (Fig. 6d).

TNBS altered ChAT expression in distal colon

ChAT immunostaining was used to investigate the alterations of enteric cholinergic neurons after TNBS treatment. We observed that scattered ChAT-positive cells were present in the mucosa layer of both control and TNBS mice, where they likely represented the tuft cells, as previously demonstrated (Casini et al. 2021), and result slightly increased after TNBS treatment (Fig. 7a). ChAT immunostaining was significantly increased also in the neurons of the myenteric

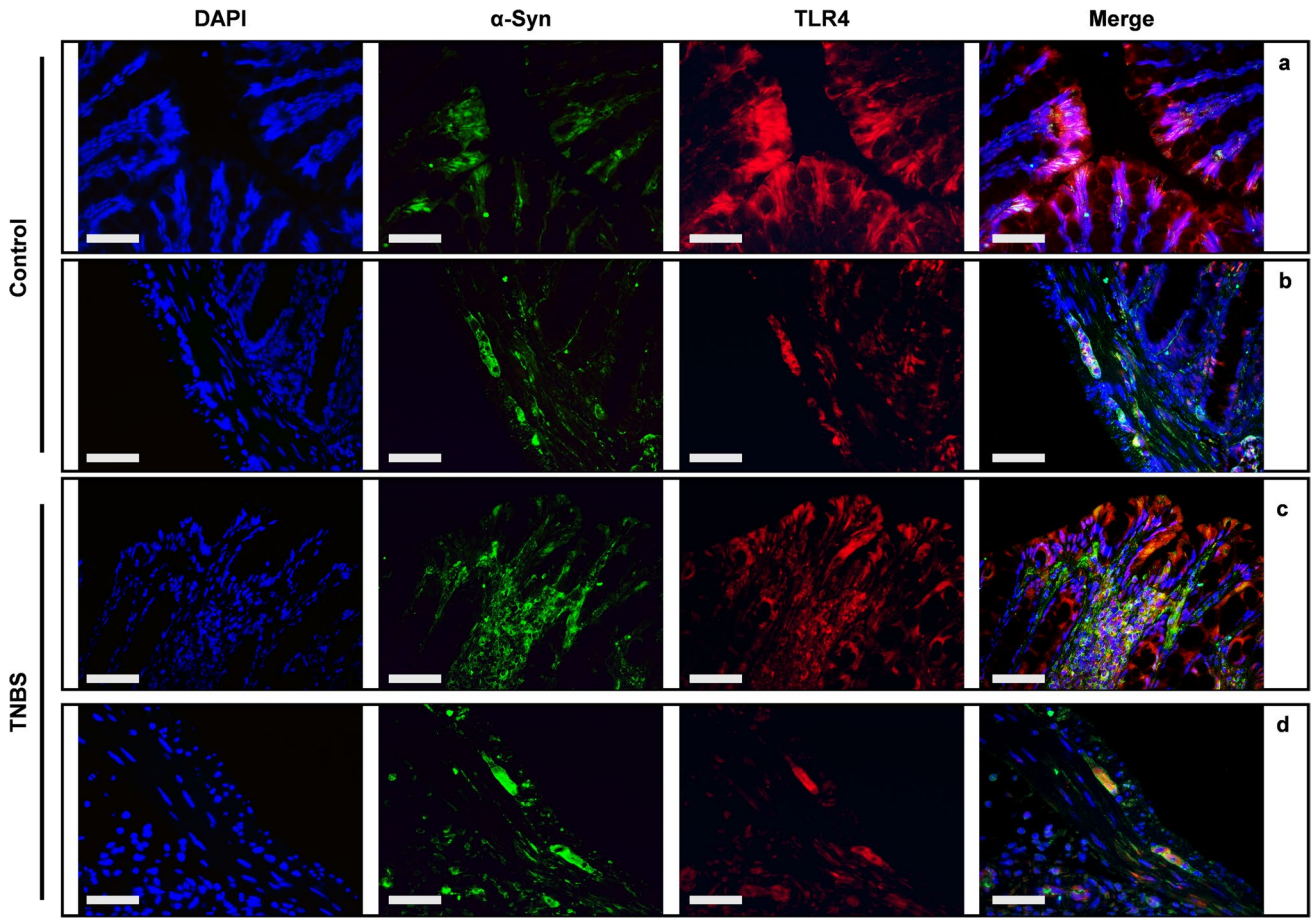

Fig. 6 Co-expression of α-syn and TLR4 in the colon of TNBS-induced colitis double IF with anti α-syn and anti-TLR4 antibodies in the mucosa (**a** and **c**) and in the muscularis externa (**b** and **d**) of control and TNBS-treated mice. An extensive co-expression between TLR4 and α-syn is detectable in TNBS-treated mice, in both mucosal layer and myenteric plexus. OM 40 × scale bars = 50 μm

plexus of TNBS-treated mice, in comparison to control mice, indicating that cholinergic transmission may increase after TNBS treatment and colon inflammation (Fig. 7b). The double IF labeling did not reveal any co-expression between ChAT and α-syn in the mucosa of control mice (Fig. 8a), whereas a strong co-expression was detected in myenteric ganglia (Fig. 8b). Colocalization between ChAT and α-syn was increased by TNBS treatment both in the tuft cells of the mucosa (Fig. 8c) and in the myenteric neurons (Fig. 8d), suggesting an increased expression of α-syn in cholinergic neurons, due to an inflammatory phenotype.

TNBS altered the expression of VIP and TH in distal colon

Cytological changes in myenteric motor-neurons were investigated by VIP immunostaining. TNBS treatment significantly increased the expression of VIP in the mucosa of the distal colon (Fig. 9a). VIP-immunoreactivity was present in the ganglia of the myenteric plexus and in nerve fibers innervating the mucosa with a punctuated and various patterns. Furthermore, we observed a trend toward increase of VIP-ir in the ganglia of the myenteric plexus of TNBS-treated mice (Fig. 9b). Double IF demonstrated that VIP and α-syn co-expressed in the myenteric plexus but not in the mucosa of control mice (Fig. 10a), whereas colocalization between VIP and α-syn is detected in the neurons of the myenteric plexus (Fig. 10b). After TNBS treatment, co-expression between VIP and α-syn was significantly increased, both in the neuronal fibers around mucosal cells, as in the neurons of the myenteric plexus (Fig. 10c, d).

To better characterize the changes in the enteric neurons, after TNBS treatment, we investigated the expression of TH as a marker of dopaminergic and catecholaminergic neurons (Daubner, et al. 2011). Control mice and TNBS-treated mice disclose evident differences in TH immunoreactivity in the mucosa and lamina propria of the distal colon. In the mucosa and lamina propria, TH-ir was higher (although not significantly) in neuronal processes of control mice, compared to TNBS-treated mice, with dense varicose

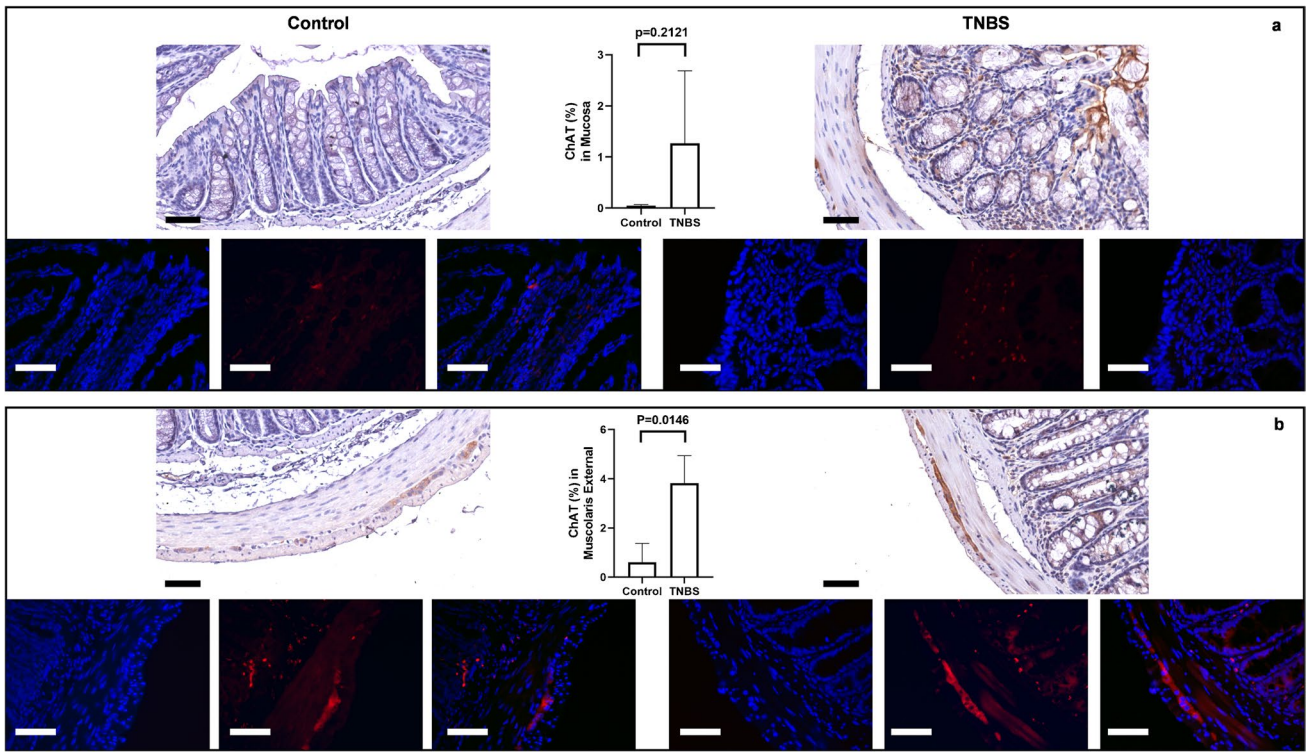

Fig. 7 TNBS treatment alters the ChAT expression in both mucosal and muscular layer. (**a**) ChAT expression is present in scattered mucosa cells of control mice and increases in the fibers around mucosal gland and in the submucosa of TNBS-treated mice, as revealed by quantitative analysis. *SD* of control = 0.01862; *SD* of TNBS = 1.42; *p*-value = 0.2121. (**b**) In the muscularis externa, ChAT is slightly expressed in the myenteric neurons of control mice, where it is drastically increased after TNBS treatment. *SD* of control = 0.7642; *SD* of TNBS = 1.115; *p*-value = 0.0146. OM 40× scale bars = 50 µm

fibers observable in both transverse and longitudinal sections and likely belonging to Meissner's plexus (Fig. 11a). Similarly, a significantly lower expression of TH was observed in the ganglia of the myenteric plexus, after TNBS treatment (Fig. 11b). To characterize the neuron population and their changes during TNBS treatment in the distal colon, we measured the expression of TH enzyme as it is found in dopaminergic, adrenergic, and noradrenergic neurons (Daubner et al. 2011). Control and TNBS mice showed changes in TH immunoreactivity in the mucosa of the distal colon (Fig. 11a). In the Auerbach's plexus of control mice, TH-ir was significant higher in neuronal processes with dense varicose fibers observable by both transverse and longitudinal sections. Lower expression of TH-ir in neuronal cell bodies and processes was observed in TNBS-treated mice (Fig. 11b). Quantification of myenteric plexus ganglia confirmed catecholaminergic loss. In the mucosa and submucosa layers, TH-ir was abundant in glandular ducts and rarer around blood vessels and in epithelial cells of control mice, whereas we found a decrease in the epithelium and in plexa after TNBS treatment.

TNBS reduced CGRP/CALCRL axis in the distal colon

Different studies have shown that CGRP plays a crucial role in many physiological and pathological functions of the ENS, including the regulation of GI smooth muscle mobility (Chiocchetti, et al. 2006; Kawasaki 2002), and the stimulation of mucus secretion after nociceptor activation (Yang, et al. 2022). CGRP and its receptor (CALCR) are highly expressed by intrinsic primary afferent enteric neurons (IPAN) (Hibberd et al. 2022). After TNBS treatment, CGRP was reduced in the various fibers innervating the glands and the lamina propria of the distal colon (Fig. 12a), while — in the same animals — a significant reduction of CGRP-positive neurons was detected in the ganglia of the myenteric plexus, in comparison to control mice (Fig. 12b). Surprisingly, neither significative difference nor a decreasing trend was found in the expression of CALCRL ($p = 0.261$) in the mucosa of TNBS-treated mice, in comparison to control mice (Fig. 12c), whereas, after TNBS treatment, the expression of the CGRP receptor was significantly decreased in the ganglia of the myenteric plexus (Fig. 12d). Interestingly, we observed a different distribution of CGRP

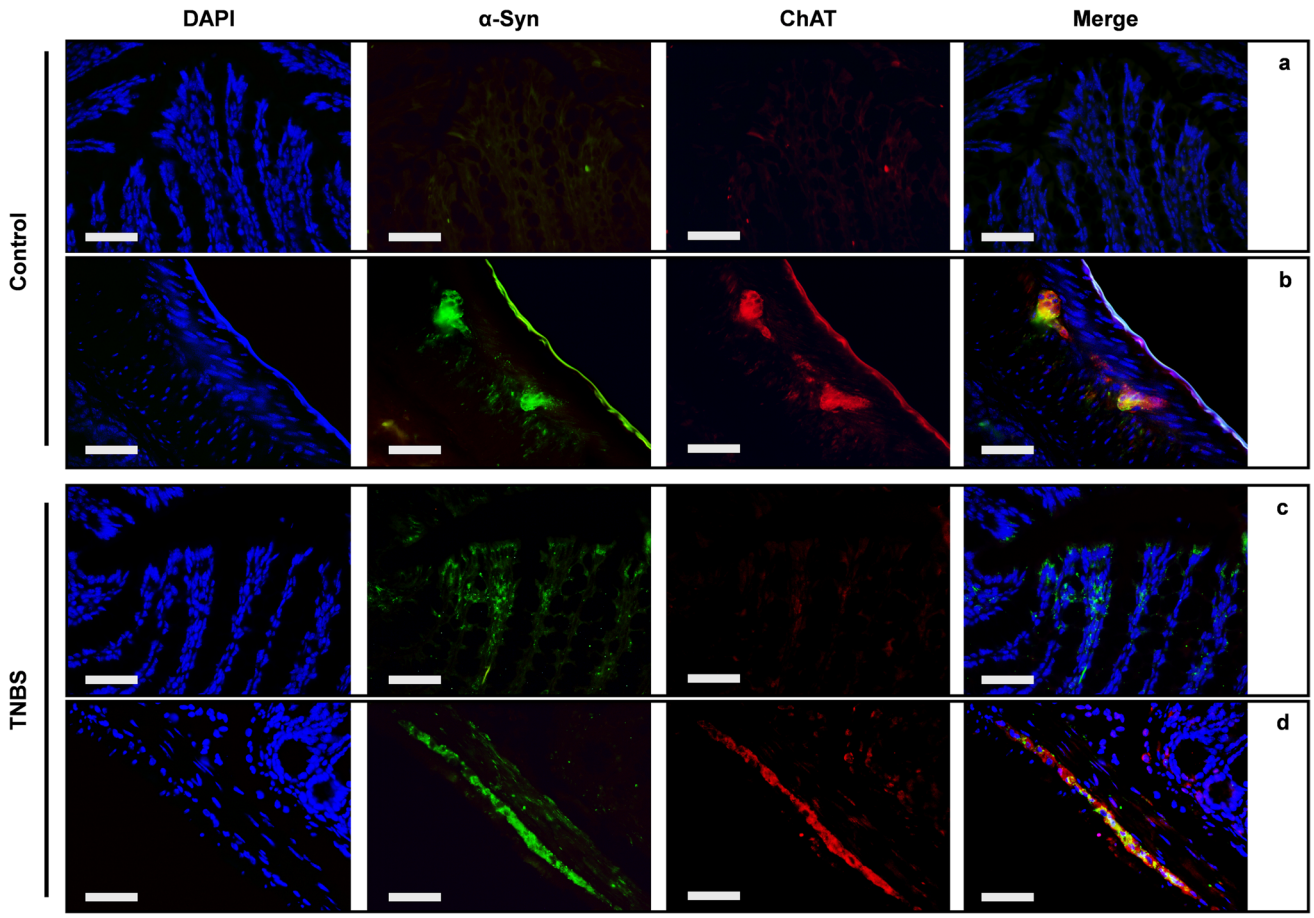

Fig. 8 α-Syn and ChAT are co-expressed in both mucosa and myenteric plexus. In control mice, co-expression between ChAT (red) and α-syn (green) was very week in mucosal layer (**a**). Whereas an extensive co-expression (merge — yellow) was detected in the myenteric neurons (**b**). Slightly increased co-expression of ChAT and α-syn (merge — yellow) features the mucosa and the lamina propria of TNBS-treated colon (**c**). While a wide co-expression is constantly detected in the myenteric plexus (**d**). OM 40 × scale bars = 50 µm

and CALCRL in the distal colon of TNBS-treated mice in comparison to control mice. CALCRL was mostly expressed by goblet cells in both control and TNBS-treated mice, while it was also expressed by neuronal cells of the mucosal plexus of Meissner in control mice. Conversely, the expression of CGRP was evident in neuroendocrine cells, myenteric neurons and goblet cells of control mice, whereas it became prevalent in the inflammatory infiltrate in TNBS-treated mice (Fig. 12a, b).

Discussion

In the present study, we investigated the architecture and the histomorphology of the distal colon after treatment with the pro-inflammatory toxin TNBS, highlighting the connection between intestinal inflammation and aggregation of α-syn. As expected, we find that the inflammatory infiltrate was significantly increased in the colon of TNBS-treated mice with respect to control mice and that — in the same animals — the morphology and the number of different mucous-secreting cells were profoundly altered. α-Syn expression was significantly increased in the submucosal plexus and in the mucosa of TNBS-treated mice and interestingly, pS129 α-syn aggregates, with amyloid conformation, were detected in the inflammatory infiltrate around colonic glands and co-expressed with macrophage markers. TNBS treatment modified the entire architecture of the enteric nervous and neuroendocrine systems: ChAT expression increased in the neurons of the myenteric plexus, along within the tuft cells and the neuronal fibers innervating the mucosa. Similarly, VIP increased in the neurons of the myenteric plexus in the submucosal Auerbach's plexus and in the neuronal fibers innervating mucosal glands. Differently, TH significantly decreased after TNBS treatment either in the muscularis externa or in the mucosa, along with CGRP and its receptor CALCRL, which were either decreased as differentially expressed in the colonic wall of TNBS treated mice.

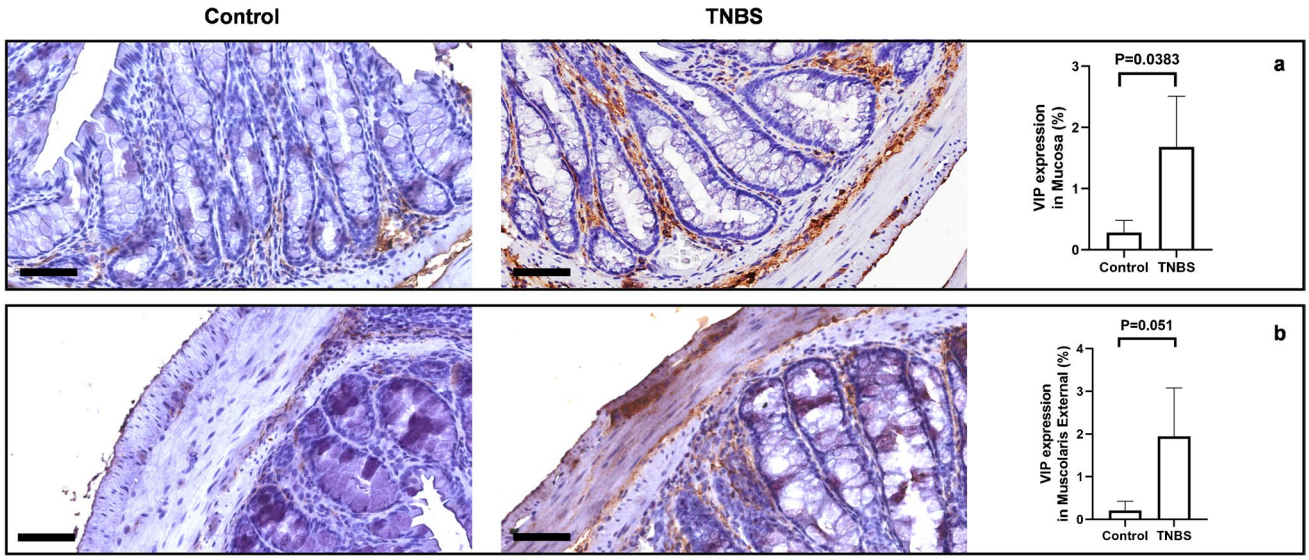

Fig. 9 VIP expression is increased in TNBS-treated mice. (**a**) VIP is expressed by scattered mucosal cells and by submucosal neurons of control mice. Increased expression of VIP is detected in the submucosal plexus and in the fibers innervating the mucosal glands, after treatment with TNBS. *SD* of control = 0.197; *SD* of TNBS = 0.83; *p*-value = 0.0383. (**b**) A similar profile is detectable in the muscularis externa, where VIP is almost unexpressed in the myenteric neurons of control mice, while it dramatically increases in the same neurons after TNBS treatment. *SD* of control = 0.218; *SD* of TNBS = 1.133; *p*-value = 0.051. OM 40 × scale bars = 50 µm

As previously demonstrated, TNBS can promote a profound alteration of the colonic wall, inducing injuries at the colonic epithelium, increasing mucosal permeability and producing hyperemia and mucosal ulceration, with the consequent development of acute and chronic inflammation (Palmen, et al. 1995; Tatsumi and Lichtenberger 1996; Yamada, et al. 1992). This was confirmed in our study by the increased inflammatory score that we detected in the colon of TNBS-treated mice. Similarly, goblet cells secreting mucins that form the mucous layer, functioning as first line protection from injuries and imbalanced microbial population (Johansson and Hansson 2016), were altered after TNBS treatment, as detected by both PAS and Alcian-blue staining. Previous studies demonstrated that alteration of goblet cells is invariably present in both experimental and human colitis, and it contributes to the early stages of UC, in which the damage of intestinal mucous barrier precedes the inflammatory infiltration (Boltin, et al. 2013; Johansson, et al. 2010). Moreover, active UC is featured by the loss of goblet cells and the compromising of mucous layer composition (Singh, et al. 2022). In agreement with our results, showing loss of both PAS and Alcian-blue positive goblet cells, acidic and neutral mucin secretion are likely altered in TNBS-induced colitis.

The most relevant finding of our morphological study was the increased expression of α-syn in the colonic mucosa of TNBS-treated mice and the formation of pS129 α-syn aggregates in the neuronal plexa and in the macrophages of the inflammatory infiltrate. Lewy pathology has been detected in the colon of patients with PD, together with the elevation of pro-inflammatory cytokines (Devos, et al. 2013). Similarly, in patients with UC, previous studies have demonstrated the presence of pS129 α-syn aggregates in myenteric and submucosal neurons and in neuronal fibers innervating smooth muscular cells and mucous glands (Gibo, et al. 2022). Our findings agree with these pathological observations and support the intertwined relation between α-syn accumulation and bowel inflammation. Moreover, they replicate — for the first time in TNBS-induced colitis — what was already observed in experimental colitis obtained by the administration of dextran-sulfate (DSS) in both mice (Grathwohl, et al. 2021, Kishimoto, et al. 2019) and non-human primates (Resnikoff, et al. 2019). In previous experimental studies, pS129 α-syn was found increased in myenteric neurons after treatment with DSS, while not phosphorylated (native) α-syn resulted reduced (Prigent, et al. 2019a). In our study, we detected a dramatic increase in α-syn staining in the mucosa, with both native α-syn antibody and pS129 α-syn antibody, while only pS129 α-syn antibody detected changes in the myenteric neurons. α-Syn expression in the mucosa and in the inflammatory infiltrate was not investigated in other studies and presumably — in myenteric neurons — the formation of pS129 α-syn aggregates is responsible of sequestering monomeric α-syn, thereby reducing the widespread staining with native α-syn antibodies. Further studies are needed to distinguish the effect of acute and chronic TNBS

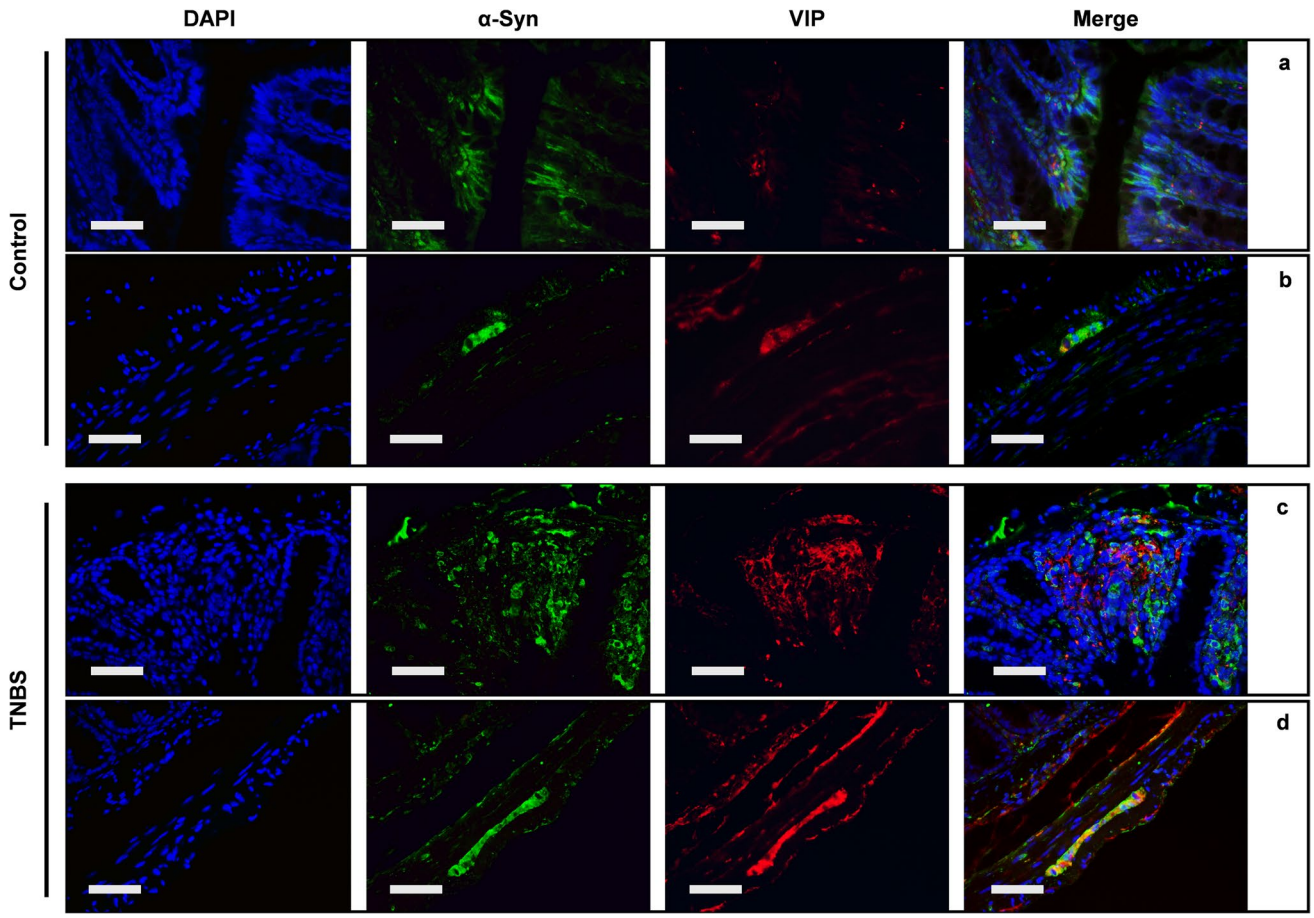

Fig. 10 α-Syn and VIP are co-expressed both in mucosa and myenteric plexus of TNBS-treated mice double IF for α-syn (green) and VIP (red). Expression of both VIP and α-syn is increased in the mucosa and in the submucosal plexus of TNBS-treated mice (**c**), in comparison to control mice (**a**). Co-expression is detected in the fibers gathering the mucosal glands and the inflammatory infiltrate of TNBS-treated mice. Similarly, increased VIP expression is detected in the myenteric ganglia of TNBS-treated mice (**d**), in comparison to control mice (**b**) and extensive co-expression between VIP and α-syn is evident in myenteric neurons, after TNBS treatment. OM 40×

treatment, since different patterns of α-syn expression have been detected in acute, rather than chronic DSS-induced colitis (Grathwohl et al. 2021, Lin, et al. 2022, Prigent et al. 2019a). As a novel interesting finding, pS129 α-syn aggregates with amyloid conformation — as proved by ThT staining — were detected in the inflammatory cells infiltrating both mucosa and submucosa of TNBS-treated mice, and they were co-expressed with the pan-macrophagic marker F4/80. Amyloid aggregates of α-syn are likely responsible for inter-neuronal spreading of α-syn pathology in the ENS and from the enteric neurons to the brain (Chandra, et al. 2023, Zampar, et al. 2024). Moreover, the activation of TLRs by α-syn oligomers is in charge to produce inflammatory cytokines, towards the activation of the NFkB pathway (Conte, et al. 2023, Heidari, et al. 2022; Hughes, et al. 2019). Accordantly, we found an increased colocalization between α-syn and TLR4 in both mucosa and myenteric neurons of TNBS-treated mice, morphologically supporting the interaction between α-syn aggregates and TLR4, which has been shown to drive neuroinflammation also in PD (Fellner, et al. 2013, Yoon, et al. 2023).

Macrophages and natural killer (NK) cells internalize α-syn aggregates by phagocytosis, degrading toxic α-syn species (Matveyenka, et al. 2024). However, an increased internalization of α-syn oligomers can induce endo-lysosomal stress and phagocytic dysfunction, leading to the progression of α-syn pathology in the ENS (Mackie, et al. 2023). Our morphological evidence supports the importance of macrophage-neuron interaction in removing protein aggregates from the ENS, which putatively shape the early stages of synucleinopathies in the enteric neurons. Furthermore, a recent study on a brain-first model of PD, demonstrates that activated mononuclear cells (CD11c + macrophages) were responsible for the spreading of α-syn aggregates from the brain to the ileum (McFleder, et al. 2023). Our results, highlighting the engulfment of pS129 α-syn aggregates by enteric macrophages, support a hypothetical role of gut mononuclear cells in the trafficking of α-syn from the gut to the brain,

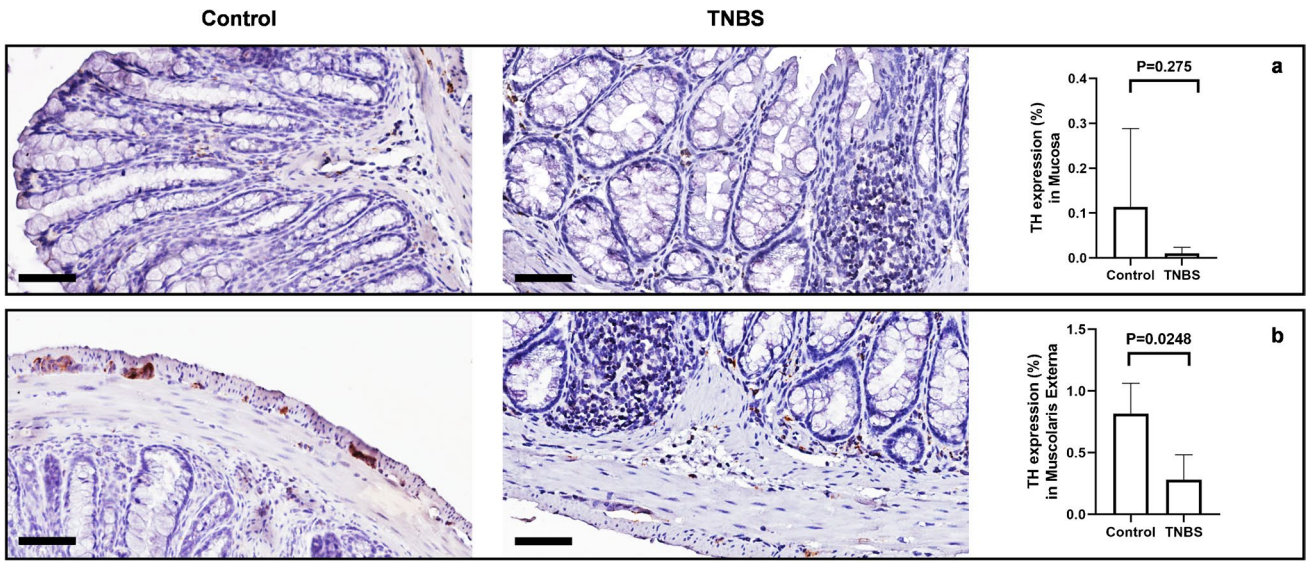

Fig. 11 TNBS-treated mice show decreased TH expression in myenteric plexuses. (**a**) TH expression was slightly weak in the mucosa and the submucosa, and no significant changes in TH-immunoreactivity in the mucosa were detectable between controls and TNBS-treated mice. *SD* of control = 0.1748; *SD* of TNBS = 0.0138; *p*-value = 0.275. (**b**) In control mice, TH is highly expressed by sparse neurons of myenteric plexus. After TNBS treatment, a significant loss of TH-positive enteric neurons is detectable. *SD* of control = 0.246; *SD* of TNBS = 0.201; *p*-value = 0.0248. OM 40 × scale bars = 50 µm

as likely occurs in body first PD (Borghammer, et al. 2021, Braak, et al. 2006, Braak, et al. 2003).

As expected, the entire ENS was affected by TNBS treatment. Increased levels of ChAT were detected in both myenteric and submucosal neurons as well as neuronal fibers gathering the mucosal layer. ChAT + neurons represent a major component of the ENS (Mazzoni, et al. 2021). They are mostly effector neurons, responsible for motility and secretion (Foong, et al. 2014; Fornai, et al. 2016). Increased ChAT expression after TNBS treatment may reflect an increased firing of cholinergic enteric neurons, which drives the increased secretory and peristaltic activity, featuring colon inflammation. Recent studies have also demonstrated that cholinergic transmission protects from inflammatory damage by modulating macrophages towards an anti-inflammatory phenotype, with production of IL-10 and IL-22 (Populin, et al. 2021, Zheng, et al. 2021). Our morphological data suggest a possible compensatory mechanism of increasing cholinergic transmission, aimed at rescuing inflammatory injuries during colitis.

Similarly, we can interpret the increased expression of VIP in both mucosa and muscularis externa. In physiological conditions, VIP + neurons are mainly localized in the submucosal plexus, where they mostly act as secretory-driving neurons, innervating mucosal glands (Chino, et al. 2002). VIP + fibers around mucosal glands are increased in patients with IBD (Rychlik, et al. 2020) and inflammatory cytokines — particularly IL-1β — increase VIP expression in both submucosal and myenteric neurons (Neunlist, et al. 2003; Tjwa, et al. 2003), probably contributing to increased secretion and hypermotility. The dramatic increase of VIP expression by myenteric neurons during inflammation may also have pro-survival and protective properties (Sandgren, et al. 2003). Previous studies have shown the homeostatic function of VIP on intestinal smooth muscle and myenteric neurons during an inflammation, through the blocking of NFkB nuclear translocation and thereby reduction of inflammatory cytokines production (Shi and Sarna 2009). Our morphological data further support this putative compensatory mechanism. Whether changes in VIP and ChAT expression are dependent on altered α-syn expression or aggregation needs to be better clarified. Previous evidence has shown α-syn pathology in VIP neurons and cholinergic terminals in the ENS of both PD patients (Annerino, et al. 2012; Wang, et al. 2012) and experimental models of parkinsonism obtained by 6-hydroxydopamine (6-OHDA) (Colucci, et al. 2012). We detected a widespread co-expression between both VIP or ChAT and α-syn, which mostly involves myenteric neurons and mucosal fibers of TNBS-treated mice. This suggests a contribution of α-syn on the alterations of the ENS during an inflammation, which is similar to that occurring at the ENS of PD patients.

Differently, TH and CGRP/CALCR were both reduced after TNBS treatment. Dopaminergic and catecholaminergic neurons are particularly sensible to oxidative stress and α-syn pathology (Vivacqua, et al. 2024). Lewy pathology has

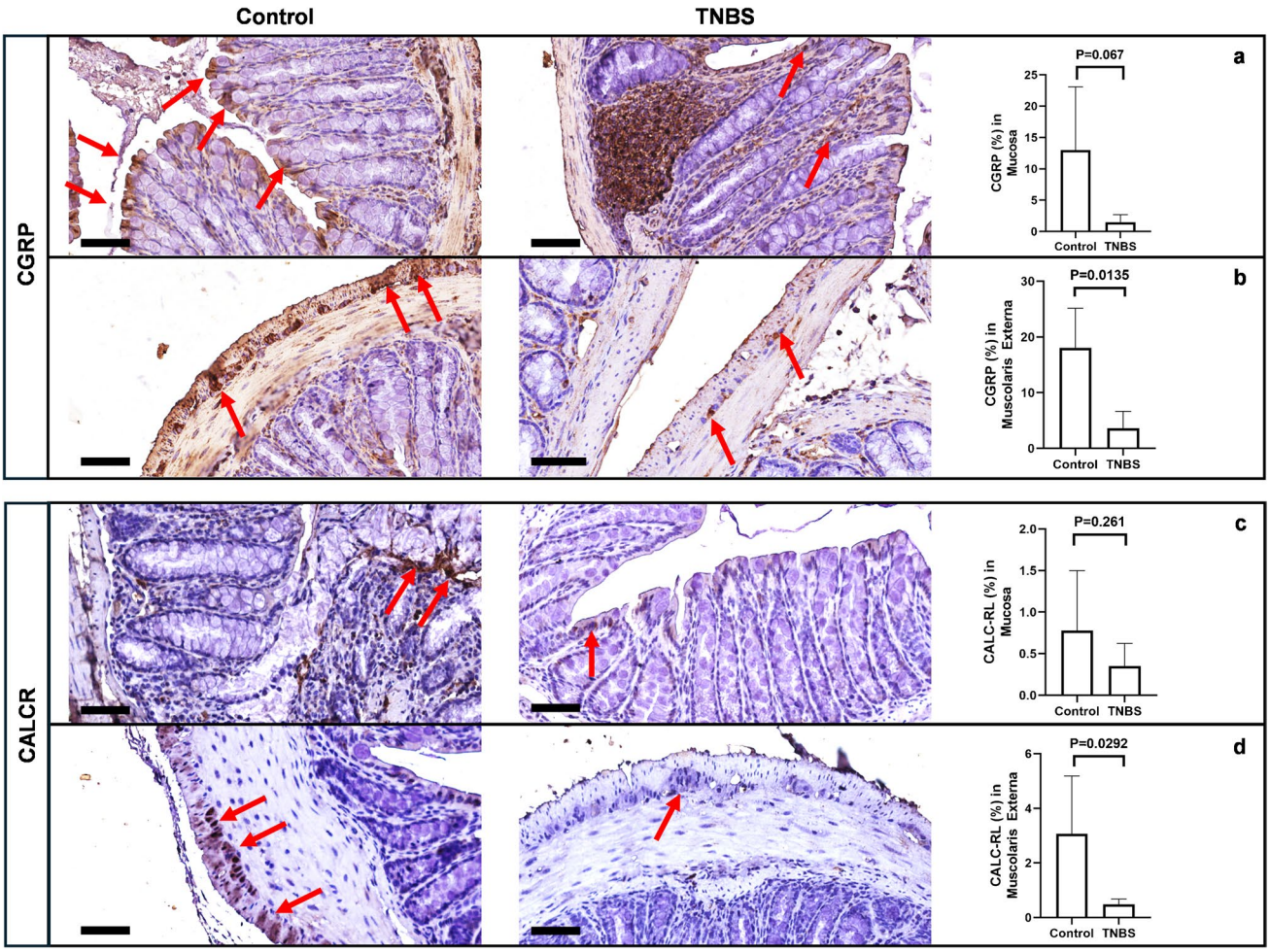

Fig. 12 CGRP and CALCRL expression are reduced in the colon of TNBS mice. (**a**) In control mice, CGRP (α and β) is expressed by the neurons of submucosal plexus, with the fibers projecting to the mucosa and gathering mucous glands (red arrows). The mucosal and submucosal expression is reduced after TNBS treatment (*SD* of control = 10.10; *SD* of TNBS = 1.218; *p*-value = 0.067), and a widespread positivity for CGRP becomes visible in the inflammatory infiltrate, at both mucosa and submucosa. (**b**) Similarly, CGRP is strongly expressed in the myenteric plexus of control mice, and a significant reduction is detectable after treatment with TNBS (red arrows). *SD* of control = 7.093; *SD* of TNBS = 3.055; *p*-value = 0.0135. (**c**) A slight but not significant reduction of CALCR expression is detected in the mucosa and the submucosa after treatment with TNBS (red arrows). *SD* of control = 0.72; *SD* of TNBS = 0.2707; *p*-value = 0.261. (**d**) In the muscularis externa, control mice express CALCR in myenteric neurons, where it results significantly reduced after treatment with TNBS (red arrows). *SD* of control = 2.125; *SD* of TNBS = 0.189; *p*-value = 0.0292. OM 40 × scale bars = 50 µm

been detected in TH + neurons of PD patients (Koeglsperger, et al. 2023; Travagli, et al. 2020). After systemic administration of the parkinsonian neurotoxin 1-methyl-4-phenyl1-1,2,3,6-tetrahydropyridine (MPTP), a synchronous loss of TH + neurons has been found in the midbrain and in the colon of primates, along with the parallel formation of α-syn oligomers in the same sites (Li, et al. 2020). While reduction of TH + neurons has been reported also in mice, treated with 6-OHDA in the midbrain, suggesting a modulatory interplay between midbrain DA system and ENS (Colucci et al. 2012). The dramatic reduction of TH expression that we reported —— in a model of experimental colitis — further supports the occurrence of common pathological mechanisms, bringing inflammation with synucleinopathies in the ENS.

CGRP and its receptor are markers of the intrinsic primary afferent neurons (IPAN) of the ENS, responsible for sensory and motor reflexes (Cottrell, et al. 2012; Hibberd et al. 2022). Alterations in IPAN likely lead to impaired enteric reflexes, contributing to dysmotility and altered secretory phenotype. CGRP neurons are altered in colon inflammation (Makowska and Gonkowski 2018). Maternal immune activation (MIA) during pregnancy, increases the risk of developing IBD, and MIA mice present hyper-susceptibility to experimental colitis, together with a profound

reduction of CGRP positive fibers in the colonic mucosa (Li, et al. 2023). Our morphological data in TNBS-treated mice support these previous observations, showing also an increased expression of CGRP in the inflammatory infiltrate of the submucosa and around mucosal glands. CGRP innervation of the lymphoid aggregates and mononuclear cells, likely has immunomodulatory effect (Li et al. 2023; Populin et al. 2021), representing a further compensatory mechanism of the ENS in the context of colitis.

In conclusion, changes in the neurochemical architecture of the ENS may play a role in the altered motility and secretory response, featuring IBD and experimental colitis. α-Syn may directly contribute to these morpho-functional alterations. Altered neuropeptides could also represent a compensatory mechanism orchestrated by the ENS to counteract inflammation. Common pathways are likely shared by inflammation and synucleinopathies at the ENS, suggesting an intertwined relation between IBD and PD.

Author contributions AC and GV planned the experiments; LC, SL, FMB, SV and EB performed experiments; RS, AV, LP and GL prepared samples and collected images; LC, SL, RV, SC, AF, and PM analyzed data; AC, GV, MT, GL, PO and RM wrote the paper; EG and RM supervised the work. All authors revised, read and approved the manuscript.

Funding This project received financial support from "Progetti medi di Ateneo 2020" of Sapienza University of Rome (PI Profs Paolo Onori, Romina Mancinelli and Eugenio Gaudio).

Data availability No datasets were generated or analysed during the current study.

Declarations

Ethics approval Ethics approval is not applicable in this study.

Conflicts of interest The authors declare no competing interests.

References

Annerino DM, Arshad S, Taylor GM, Adler CH, Beach TG, Greene JG (2012) Parkinson's disease is not associated with gastrointestinal myenteric ganglion neuron loss. Acta Neuropathol 124:665–680

Anwar S, Peters O, Millership S, Ninkina N, Doig N, Connor-Robson N, Threlfell S, Kooner G, Deacon RM, Bannerman DM, Bolam JP, Chandra SS, Cragg SJ, Wade-Martins R, Buchman VL (2011) Functional alterations to the nigrostriatal system in mice lacking all three members of the synuclein family. J Neurosci 31:7264–7274

Bechtold BJ, Lynch KD, Oyanna VO, Call MR, White LA, Graf TN, Oberlies NH, Clarke JD (2024) Pharmacokinetic effects of different models of nonalcoholic fatty liver disease in transgenic humanized OATP1B mice. Drug Metab Dispos 52:355–367

Boltin D, Perets TT, Vilkin A, Niv Y (2013) Mucin function in inflammatory bowel disease: an update. J Clin Gastroenterol 47:106–111

Bonaccorsi di Patti MC, Angiulli E, Casini A, Vaccaro R, Cioni C, Toni M (2022) Synuclein analysis in adult Xenopus laevis. Int J Mol Sci 23:6058

Borghammer P, Horsager J, Andersen K, Van Den Berge N, Raunio A, Murayama S, Parkkinen L, Myllykangas L (2021) Neuropathological evidence of body-first vs. brain-first Lewy body disease. Neurobiol Dis 161:105557

Bottner M, Fricke T, Muller M, Barrenschee M, Deuschl G, Schneider SA, Egberts JH, Becker T, Fritscher-Ravens A, Ellrichmann M, Schulz-Schaeffer WJ, Wedel T (2015) Alpha-synuclein is associated with the synaptic vesicle apparatus in the human and rat enteric nervous system. Brain Res 1614:51–59

Braak H, Rub U, Gai WP, Del Tredici K (2003) Idiopathic Parkinson's disease: possible routes by which vulnerable neuronal types may be subject to neuroinvasion by an unknown pathogen. J Neural Transm (Vienna) 110:517–536

Braak H, de Vos RA, Bohl J, Del Tredici K (2006) Gastric alpha-synuclein immunoreactive inclusions in Meissner's and Auerbach's plexuses in cases staged for Parkinson's disease-related brain pathology. Neurosci Lett 396:67–72

Brehmer A, Schrodl F, Neuhuber W (2006) Morphology of VIP/nNOS-immunoreactive myenteric neurons in the human gut. Histochem Cell Biol 125:557–565

Casini A, Mancinelli R, Mammola CL, Pannarale L, Chirletti P, Onori P, Vaccaro R (2021) Distribution of alpha-synuclein in normal human jejunum and its relations with the chemosensory and neuroendocrine system. Eur J Histochem 65(4):3310. https://doi.org/10.4081/ejh.2021.3310

Chandra R, Sokratian A, Chavez KR, King S, Swain SM, Snyder JC, West AB, Liddle RA (2023) Gut mucosal cells transfer alpha-synuclein to the vagus nerve. JCI Insight 8(23). https://doi.org/10.1172/jci.insight.172192

Cheng F, Vivacqua G, Yu S (2011) The role of alpha-synuclein in neurotransmission and synaptic plasticity. J Chem Neuroanat 42:242–248

Chino Y, Fujimura M, Kitahama K, Fujimiya M (2002) Colocalization of NO and VIP in neurons of the submucous plexus in the rat intestine. Peptides 23:2245–2250

Chiocchetti R, Grandis A, Bombardi C, Lucchi ML, Dal Lago DT, Bortolami R, Furness JB (2006) Extrinsic and intrinsic sources of calcitonin gene-related peptide immunoreactivity in the lamb ileum: a morphometric and neurochemical investigation. Cell Tissue Res 323:183–196

Colucci M, Cervio M, Faniglione M, De Angelis S, Pajoro M, Levandis G, Tassorelli C, Blandini F, Feletti F, De Giorgio R, Dellabianca A, Tonini S, Tonini M (2012) Intestinal dysmotility and enteric neurochemical changes in a Parkinson's disease rat model. Auton Neurosci 169:77–86

Conte C, Ingrassia A, Breve J, Bol JJ, Timmermans-Huisman E, van Dam AM, Beccari T, van de Berg WDJ (2023) Toll-like receptor 4 is upregulated in Parkinson's disease patients and co-localizes with pSer129alphaSyn: a possible link with the pathology. Cells 12:1368

Cottrell GS, Alemi F, Kirkland JG, Grady EF, Corvera CU, Bhargava A (2012) Localization of calcitonin receptor-like receptor (CLR) and receptor activity-modifying protein 1 (RAMP1) in human gastrointestinal tract. Peptides 35:202–211

Daubner SC, Le T, Wang S (2011) Tyrosine hydroxylase and regulation of dopamine synthesis. Arch Biochem Biophys 508:1–12

Devos D, Lebouvier T, Lardeux B, Biraud M, Rouaud T, Pouclet H, Coron E, des Varannes SB, Naveilhan P, Nguyen JM, Neunlist M, Derkinderen P (2013) Colonic inflammation in Parkinson's disease. Neurobiol Dis 50:42–48

Erben U, Loddenkemper C, Doerfel K, Spieckermann S, Haller D, Heimesaat MM, Zeitz M, Siegmund B, Kuhl AA (2014) A guide to histomorphological evaluation of intestinal inflammation in mouse models. Int J Clin Exp Pathol 7:4557–4576

Espinosa-Oliva AM, Ruiz R, Soto MS, Boza-Serrano A, Rodriguez-Perez AI, Roca-Ceballos MA, Garcia-Revilla J, Santiago M, Serres S, Economopoulus V, Carvajal AE, Vazquez-Carretero MD, Garcia-Miranda P, Klementieva O, Oliva-Martin MJ, Deierborg T, Rivas E, Sibson NR, Labandeira-Garcia JL, Machado A, Peral MJ, Herrera AJ, Venero JL, de Pablos RM (2024) Inflammatory bowel disease induces pathological alpha-synuclein aggregation in the human gut and brain. Neuropathol Appl Neurobiol 50:e12962

Fellner L, Irschick R, Schanda K, Reindl M, Klimaschewski L, Poewe W, Wenning GK, Stefanova N (2013) Toll-like receptor 4 is required for alpha-synuclein dependent activation of microglia and astroglia. Glia 61:349–360

Foong JP, Tough IR, Cox HM, Bornstein JC (2014) Properties of cholinergic and non-cholinergic submucosal neurons along the mouse colon. J Physiol 592:777–793

Fornai M, Pellegrini C, Antonioli L, Segnani C, Ippolito C, Barocelli E, Ballabeni V, Vegezzi G, Al Harraq Z, Blandini F, Levandis G, Cerri S, Blandizzi C, Bernardini N, Colucci R (2016) Enteric dysfunctions in experimental Parkinson's disease: alterations of excitatory cholinergic neurotransmission regulating colonic motility in rats. J Pharmacol Exp Ther 356:434–444

Gibo N, Hamaguchi T, Miki Y, Yamamura T, Nakaguro M, Ito M, Nakamuara M, Kawashima H, Hirayama M, Hirooka Y, Wakabayashi K, Ohno K (2022) Examination of abnormal alpha-synuclein aggregates in the enteric neural plexus in patients with ulcerative colitis. J Gastrointestin Liver Dis 31:290–300

Grathwohl S, Quansah E, Maroof N, Steiner JA, Spycher L, Benmansour F, Duran-Pacheco G, Siebourg-Polster J, Oroszlan-Szovik K, Remy H, Haenggi M, Stawiski M, Selhausen M, Mailver P, Wolfert A, Emrich T, Madaj Z, Su A, Escobar Galvis ML, Mueller C, Herrmann A, Brundin P, Britschgi M (2021) Specific immune modulation of experimental colitis drives enteric alpha-synuclein accumulation and triggers age-related Parkinson-like brain pathology. Free Neuropathol 2:2–13. https://doi.org/10.17879/freeneuropathology-2021-3326

Heidari A, Yazdanpanah N, Rezaei N (2022) The role of Toll-like receptors and neuroinflammation in Parkinson's disease. J Neuroinflammation 19:135

Hibberd TJ, Yew WP, Dodds KN, Xie Z, Travis L, Brookes SJ, Costa M, Hu H, Spencer NJ (2022) Quantification of CGRP-immunoreactive myenteric neurons in mouse colon. J Comp Neurol 530:3209–3225

Hoover JL, Bond CE, Hoover DB, Defoe DM (2014) Effect of neurturin deficiency on cholinergic and catecholaminergic innervation of the murine eye. Exp Eye Res 122:32–39

Hughes CD, Choi ML, Ryten M, Hopkins L, Drews A, Botia JA, Iljina M, Rodrigues M, Gagliano SA, Gandhi S, Bryant C, Klenerman D (2019) Picomolar concentrations of oligomeric alpha-synuclein sensitizes TLR4 to play an initiating role in Parkinson's disease pathogenesis. Acta Neuropathol 137:103–120

Johansson ME, Hansson GC (2016) Immunological aspects of intestinal mucus and mucins. Nat Rev Immunol 16:639–649

Johansson ME, Gustafsson JK, Sjoberg KE, Petersson J, Holm L, Sjovall H, Hansson GC (2010) Bacteria penetrate the inner mucus layer before inflammation in the dextran sulfate colitis model. PLoS ONE 5:e12238

Kakimoto T, Hosokawa M, Ichimura-Shimizu M, Ogawa H, Miyakami Y, Sumida S, Tsuneyama K (2023) Accumulation of alpha-synuclein in hepatocytes in nonalcoholic steatohepatitis and its usefulness in pathological diagnosis. Pathol Res Pract 247:154525

Kawasaki H (2002) Regulation of vascular function by perivascular calcitonin gene-related peptide-containing nerves. Jpn J Pharmacol 88:39–43

Kishimoto Y, Zhu W, Hosoda W, Sen JM, Mattson MP (2019) Chronic mild gut inflammation accelerates brain neuropathology and motor dysfunction in alpha-synuclein mutant mice. Neuromolecular Med 21:239–249

Koeglsperger T, Rumpf SL, Schliesser P, Struebing FL, Brendel M, Levin J, Trenkwalder C, Hoglinger GU, Herms J (2023) Neuropathology of incidental Lewy body & prodromal Parkinson's disease. Mol Neurodegener 18:32

Kurnik M, Gil K, Gajda M, Thor P, Bugajski A (2015) Neuropathic alterations of the myenteric plexus neurons following subacute intraperitoneal administration of salsolinol. Folia Histochem Cytobiol 53:49–61

Lashuel HA, Overk CR, Oueslati A, Masliah E (2013) The many faces of alpha-synuclein: from structure and toxicity to therapeutic target. Nat Rev Neurosci 14:38–48

Latella G, Vetuschi A, Sferra R, Zanninelli G, D'Angelo A, Catitti V, Caprilli R, Flanders KC, Gaudio E (2009) Smad3 loss confers resistance to the development of trinitrobenzene sulfonic acid-induced colorectal fibrosis. Eur J Clin Invest 39:145–156

Lee HJ, Suk JE, Bae EJ, Lee JH, Paik SR, Lee SJ (2008) Assembly-dependent endocytosis and clearance of extracellular alpha-synuclein. Int J Biochem Cell Biol 40:1835–1849

Li X, Yang W, Li X, Chen M, Liu C, Li J, Yu S (2020) Alpha-synuclein oligomerization and dopaminergic degeneration occur synchronously in the brain and colon of MPTP-intoxicated parkinsonian monkeys. Neurosci Lett 716:134640

Li Q, Li S, Yao Y, Ma Z, Huang C (2023) MIA mice exhibit enteric nerve defects and are more susceptible to dextran sulfate sodium-induced colitis. Brain Behav Immun 112:152–162

Lin CH, Lin HY, Ho EP, Ke YC, Cheng MF, Shiue CY, Wu CH, Liao PH, Hsu AY, Chu LA, Liu YD, Lin YH, Tai YC, Shun CT, Chiu HM, Wu MS (2022) Mild chronic colitis triggers Parkinsonism in LRRK2 mutant mice through activating TNF-alpha pathway. Mov Disord 37:745–757

Machorro-Rojas N, Sainz-Espunes T, Godinez-Victoria M, Castaneda-Sanchez JI, Campos-Rodriguez R, Pacheco-Yepez J, Drago-Serrano ME (2019) Impact of chronic immobilization stress on parameters of colonic homeostasis in BALB/c mice. Mol Med Rep 20:2083–2090

Mackie PM, Koshy J, Bhogade M, Hammoor T, Hachmeister W, Lloyd GM, Paterno G, Bolen M, Tansey MG, Giasson BI, Khoshbouei H (2023) Complement C1q-dependent engulfment of alpha-synuclein induces ENS-resident macrophage exhaustion and accelerates Parkinson's-like gut pathology. bioRxiv

Makowska K, Gonkowski S (2018) The influence of inflammation and nerve damage on the neurochemical characterization of calcitonin gene-related peptide-like immunoreactive (CGRP-LI) neurons in the enteric nervous system of the porcine descending colon. Int J Mol Sci 19:548

Matveyenka M, Zhaliazka K, Kurouski D (2024) Macrophages and natural killers degrade alpha-synuclein aggregates. Mol Pharm 21:2565–2576

Mazzoni M, Caremoli F, Cabanillas L, de Los SJ, Million M, Larauche M, Clavenzani P, De Giorgio R, Sternini C (2021) Quantitative analysis of enteric neurons containing choline acetyltransferase and nitric oxide synthase immunoreactivities in the submucosal and myenteric plexuses of the porcine colon. Cell Tissue Res 383:645–654

McFleder RL, Makhotkina A, Groh J, Keber U, Imdahl F, Pena Mosca J, Peteranderl A, Wu J, Tabuchi S, Hoffmann J, Karl AK, Pagenstecher A, Vogel J, Beilhack A, Koprich JB, Brotchie JM, Saliba AE, Volkmann J, Ip CW (2023) Brain-to-gut trafficking of alpha-synuclein by CD11c(+) cells in a mouse model of Parkinson's disease. Nat Commun 14:7529

Middleton ER, Rhoades E (2010) Effects of curvature and composition on alpha-synuclein binding to lipid vesicles. Biophys J 99:2279–2288

Neunlist M, Barouk J, Michel K, Just I, Oreshkova T, Schemann M, Galmiche JP (2003) Toxin B of Clostridium difficile activates human VIP submucosal neurons, in part via an IL-1beta-dependent pathway. Am J Physiol Gastrointest Liver Physiol 285:G1049-1055

Nishitani T, Mitoh Y, Yajima T, Tachiya D, Hoshika T, Fukunaga T, Nishitani Y, Yoshida R, Mizoguchi I, Ichikawa H, Sato T (2024) Distribution of alpha-synuclein in rat salivary glands. Anat Rec (Hoboken) 307:2933–2946

Palmen MJ, Dieleman LA, van der Ende MB, Uyterlinde A, Pena AS, Meuwissen SG, van Rees EP (1995) Non-lymphoid and lymphoid cells in acute, chronic and relapsing experimental colitis. Clin Exp Immunol 99:226–232

Populin L, Stebbing MJ, Furness JB (2021) Neuronal regulation of the gut immune system and neuromodulation for treating inflammatory bowel disease. FASEB Bioadv 3:953–966

Prigent A, Gonzales J, Durand T, Le Berre-Scoul C, Rolli-Derkinderen M, Neunlist M, Derkinderen P (2019a) Acute inflammation down-regulates alpha-synuclein expression in enteric neurons. J Neurochem 148:746–760

Prigent A, Lionnet A, Durieu E, Chapelet G, Bourreille A, Neunlist M, Rolli-Derkinderen M, Derkinderen P (2019b) Enteric alpha-synuclein expression is increased in Crohn's disease. Acta Neuropathol 137:359–361

Resnikoff H, Metzger JM, Lopez M, Bondarenko V, Mejia A, Simmons HA, Emborg ME (2019) Colonic inflammation affects myenteric alpha-synuclein in nonhuman primates. J Inflamm Res 12:113–126

Rychlik A, Gonkowski S, Calka J, Makowska K (2020) Vasoactive intestinal polypeptide (VIP) in the intestinal mucosal nerve fibers in dogs with inflammatory bowel disease. Animals (Basel) 10:1759

Sandgren K, Lin Z, Ekblad E (2003) Differential effects of VIP and PACAP on survival of cultured adult rat myenteric neurons. Regul Pept 111:211–217

Shao QH, Yan WF, Zhang Z, Ma KL, Peng SY, Cao YL, Yuan YH, Chen NH (2019) Nurr1: A vital participant in the TLR4-NF-kappaB signal pathway stimulated by alpha-synuclein in BV-2 cells. Neuropharmacology 144:388–399

Shi XZ, Sarna SK (2009) Homeostatic and therapeutic roles of VIP in smooth muscle function: myo-neuroimmune interactions. Am J Physiol Gastrointest Liver Physiol 297:G716-725

Singh V, Johnson K, Yin J, Lee S, Lin R, Yu H, In J, Foulke-Abel J, Zachos NC, Donowitz M, Rong Y (2022) Chronic inflammation in ulcerative colitis causes long-term changes in goblet cell function. Cell Mol Gastroenterol Hepatol 13:219–232

Spillantini MG, Goedert M (2018) Neurodegeneration and the ordered assembly of alpha-synuclein. Cell Tissue Res 373:137–148

Tatsumi Y, Lichtenberger LM (1996) Molecular association of trinitrobenzenesulfonic acid and surface phospholipids in the development of colitis in rats. Gastroenterology 110:780–789

Tjwa ET, Bradley JM, Keenan CM, Kroese AB, Sharkey KA (2003) Interleukin-1beta activates specific populations of enteric neurons and enteric glia in the guinea pig ileum and colon. Am J Physiol Gastrointest Liver Physiol 285:G1268-1276

Travagli RA, Browning KN, Camilleri M (2020) Parkinson disease and the gut: new insights into pathogenesis and clinical relevance. Nat Rev Gastroenterol Hepatol 17:673–685

Vaccaro R, Severi C, Serra G, Carabotti M, Casini A, Chirletti P, Onori P (2016) Endocrine cells distribution in human proximal small intestine: an immunohistochemical and morphometrical study. Ital J Anat Embryol 121:112–121

Vaccaro R, Casini A, Severi C, Lamazza A, Pronio A, Palma R (2023) Serotonin and melatonin in human lower gastrointestinal tract. Diagnostics (Basel) 13:204

Van Den Berge N, Ferreira N, Gram H, Mikkelsen TW, Alstrup AKO, Casadei N, Tsung-Pin P, Riess O, Nyengaard JR, Tamguney G, Jensen PH, Borghammer P (2019) Evidence for bidirectional and trans-synaptic parasympathetic and sympathetic propagation of alpha-synuclein in rats. Acta Neuropathol 138:535–550

Vivacqua G, Renzi A, Carpino G, Franchitto A, Gaudio E (2014) Expression of brain derivated neurotrophic factor and of its receptors: TrKB and p75NT in normal and bile duct ligated rat liver. Ital J Anat Embryol 119:111–129

Vivacqua G, Latorre A, Suppa A, Nardi M, Pietracupa S, Mancinelli R, Fabbrini G, Colosimo C, Gaudio E, Berardelli A (2016) Abnormal salivary total and oligomeric alpha-synuclein in Parkinson's Disease. PLoS ONE 11:e0151156

Vivacqua G, Suppa A, Mancinelli R, Belvisi D, Fabbrini A, Costanzo M, Formica A, Onori P, Fabbrini G, Berardelli A (2019) Salivary alpha-synuclein in the diagnosis of Parkinson's disease and progressive supranuclear palsy. Parkinsonism Relat Disord 63:143–148

Vivacqua G, Mancinelli R, Leone S, Vaccaro R, Garro L, Carotti S, Ceci L, Onori P, Pannarale L, Franchitto A, Gaudio E, Casini A (2024) Endoplasmic reticulum stress: a possible connection between intestinal inflammation and neurodegenerative disorders. Neurogastroenterol Motil 36:e14780

Wang L, Magen I, Yuan PQ, Subramaniam SR, Richter F, Chesselet MF, Tache Y (2012) Mice overexpressing wild-type human alpha-synuclein display alterations in colonic myenteric ganglia and defecation. Neurogastroenterol Motil 24:e425-436

Woerman AL, Watts JC, Aoyagi A, Giles K, Middleton LT, Prusiner SB (2018) alpha-Synuclein: multiple system atrophy prions. Cold Spring Harb Perspect Med 8:a024588

Yamada Y, Marshall S, Specian RD, Grisham MB (1992) A comparative analysis of two models of colitis in rats. Gastroenterology 102:1524–1534

Yang D, Jacobson A, Meerschaert KA, Sifakis JJ, Wu M, Chen X, Yang T, Zhou Y, Anekal PV, Rucker RA, Sharma D, Sontheimer-Phelps A, Wu GS, Deng L, Anderson MD, Choi S, Neel D, Lee N, Kasper DL, Jabri B, Huh JR, Johansson M, Thiagarajah JR, Riesenfeld SJ, Chiu IM (2022) Nociceptor neurons direct goblet cells via a CGRP-RAMP1 axis to drive mucus production and gut barrier protection. Cell 185(4190–4205):e4125

Yoon SH, Kim GY, Choi GT, Do JT (2023) Organ abnormalities caused by Turner Syndrome. Cells 12:1365

Zampar S, Di Gregorio SE, Grimmer G, Watts JC, Ingelsson M (2024) "Prion-like" seeding and propagation of oligomeric protein assemblies in neurodegenerative disorders. Front Neurosci 18:1436262

Zhang S, Liu YQ, Jia C, Lim YJ, Feng G, Xu E, Long H, Kimura Y, Tao Y, Zhao C, Wang C, Liu Z, Hu JJ, Ma MR, Liu Z, Jiang L, Li D, Wang R, Dawson VL, Dawson TM, Li YM, Mao X, Liu C (2021) Mechanistic basis for receptor-mediated pathological

alpha-synuclein fibril cell-to-cell transmission in Parkinson's disease. Proc Natl Acad Sci U S A 118:e2011196118

Zheng W, Song H, Luo Z, Wu H, Chen L, Wang Y, Cui H, Zhang Y, Wang B, Li W, Liu Y, Zhang J, Chu Y, Luo F, Liu J (2021) Acetylcholine ameliorates colitis by promoting IL-10 secretion of monocytic myeloid-derived suppressor cells through the nAChR/ERK pathway. Proc Natl Acad Sci U S A 118:e2017762118